Selection of a technique to separate carbon dioxide from methane for recovery of natural gas at Lake Kivu

MSc (50/50) RESEARCH REPORT

Prepared by

Hermann Ekini Ntini

0512451Y

Submitted to

School of Chemical and Metallurgical Engineering, Faculty of Engineering and the Built Environment, University of the Witwatersrand, Johannesburg, South Africa

Supervisor(s):

Professor Diakanua Nkazi
Dr. Elie Mukaya

November 2023

Declaration

I hereby declare that this Research Report entitled "***Selection of a technique to separate carbon dioxide from methane for recovery of natural gas at Lake Kivu"*** was written by me.

The review of the published documentations, the simulation and its discussions were put forth based on my understanding and analysis. This research report was not submitted for any degree before, either in this or in any other Universities. All used ideas were acknowledged at the respective place in the text.

Signed by:Hermann Ntini
Signed at:2023-11-30 09:05:54 +02:00
Reason:I approve

Hermann Ntini

__ _____

Hermann Ekini Ntini

(Student Number: 0512451Y)

Acknowledgement

I would like to express my deep feelings of gratitude to the late Professor Diakanua Nkazi and to Doctor Elie Mukaya for the guidance and support received during this research.

I would like to recognize my family Delphin Kadim Ntini, Modestine Yalankay Ngolo, Carine Sesep, Ayel-e-Nziam Manuella-Michelle Ntini, Nathanael Ekini Sesep Ntini and Malaika-Sabine Yalankay Ntini for their faith in me and sacrifices made towards the completion of this study.

Abstract

Lake Kivu is situated between the Democratic Republic of Congo (DRC) and Rwanda. It is known to contain large amount of dissolved carbon dioxide and methane. It is termed a killer Lake due to the toxic nature of these gases, which could emerge on the surface during a catastrophic eruption and cause massive devastation in this region. Extracting these toxic gases proves to be crucial to avoid natural disasters and to afford economic benefits in the form of electricity generation or energy export.

Table of Contents

List of Figures

List of Tables

List of abbreviations

Aspen Plus V12 – Aspen Plus Version 12

CEPCI – Chemical Plant Cost Index

CH_4 – Methane

CO_2 – Carbon dioxide

DRC – Democratic Republic of Congo

ENRTL-SR – Electrolyte non-random two liquid thermodynamic model with Soave-Redlich with Soave-Redlich equation of state

H2O – Water

KPI – Kibuye Power Limited Stage 1

PSA – Pressure swing adsorption

SRK – Soave Redlich Kwong

TSA – Temperature swings adsorption

VPSA – Vacuum pressure swing adsorption

1 INTRODUCTION

Lake Kivu situated between the Democratic Republic of Congo (DRC) and Rwanda, along with Lake Monoun and Lake Nyos in Cameroun, are three continental unique water systems due to their high content of dissolved carbon dioxide in deep water [1],[2],[30]. In Lake Kivu, the estimated volume of dissolved gases is about 300 km^3 of carbon dioxide and about 60 km^3 of methane [1],[30]. Catastrophic limnic eruptions, where large clouds of carbon dioxide were released from deep waters have occurred at Lakes Monoun and Nyos in Cameroun in a recent past leading to the killing of thousands of human lives and decimation of ecosystems around both Lakes [1],[30] .

Lake Kivu particularly contains much larger amount of dissolved methane along with carbon dioxide in deep water. Degassing of the Lake by industrial processes is a lifesaving precaution but may still pose a concern on global warming due to the potential for venting of greenhouse gases into the atmosphere.

It is therefore necessary to degas the Lake but capture the carbon dioxide for storage at safer location or for other uses. The high purity methane recovered may be used for electricity generation or commercialized as natural gas for exportation.

Three separation techniques have been shortlisted as strong candidates for recover methane from carbon dioxide at Lake Kivu [3]:

- absorption of carbon dioxide in an alkaline solution of mixed salt,
- adsorption of carbon dioxide on activated carbon,
- cold separation of carbon dioxide in liquid form.

The aim of this study was therefore to investigate and select a gas separation technique amongst three alternatives methods of gas separation. Initial flowsheets were developed for the three techniques. The total capital investment and the annual operating costs were estimated for each flowsheet.

Separation by absorption in an alkaline solvent has proved to allow a high yield or recovery of methane in the product stream, however at an excessivecost of energy as discussed in literature [31].

Cold separation or a distillation utilizing the difference in dew point between carbon dioxide and methane (cryogenic process) offers the benefit of a product stream with a high purity of methane. However, results obtained in this study points out that the cold separation technique is more expensive than the absorption technique with regards to the required cost of capital investment [32].

After calculations and comparison of the internal rate of return for the three flowsheets, adsorption on activated carbon has been retained as the most economically profitable route to consider for recovering methane from Lake Kivu with the intent of supplying international energy markets. Results of simulations in Aspen Plus prove that adsorption is the most cost-competitive amongst the three techniques when recovering methane from reservoir formations of high content of carbon dioxide due to its lower energy consumption and smaller plant equipment footprint [8].

The main disadvantage with adsorption in activated carbon is its lowest yield since a significant amount of methane is also adsorbed along with carbon dioxide in activated carbon [26], [Appendix B, section e]. Despite this fact, adsorption remains the most cost-effective technique recommended in this research in order to extract methane with a more favorable economic profitability from Lake Kivu.

1.1 PROBLEM STATEMENT

An initiative by Kivuwatt, is currently undertaken by a joint consortium between the government of Rwanda and private investors to degas Lake Kivu [1]. The initiative generates about 25 MW of electricity with gas recovered from the Lake at the Kibuye power station in Rwanda. The degassing rate is not currently sufficient to prevent future accumulation of dissolved gases in deep waters, therefore still needs to be substantially increased to mitigate the potential risk of a catastrophic limnic eruption, especially by maintaining safe concentration of dissolved gases below saturation levels[2].

Methane can be separated from carbon dioxide after the gas mixture has been extracted from the Lake. Methane may be further used for electricity generation or exported as natural gas. Carbon dioxide may be moved to a safer location for storage, sequestration or other uses after being separated from the extracted gas. Currently the two greenhouse gases end up in the atmosphere after degassing operations, which may affect health and life.

Improved separation processes are therefore necessary to be investigated and developed after degassing has taken place at Lake Kivu in support of global efforts for greenhouse gas reduction. Such separation steps should be designed as cost-effective to recover high purity methane for electricity generation or for exportation and high purity carbon dioxide for storage, sequestration or other uses. The separation technology thus must be selected, such that the overall process design leads to a reasonable investment cost and to profitable unit operations with low energy consumption.

1.2 RESEARCH OBJECTIVES

The aim of this study was to investigate and select a gas separation technique that can assist in methane gas production, and reducing the carbon dioxide concentration, which may emerge from solution and cause devastation to the eco-systems around the Lake. The objectives of this study were therefore:

- to conduct steady-state simulation of each separation technique in Aspen Plus V12 process simulator in order to achieve a specified purity and production rate of methane as required for natural gas export, and calculate
    - the yield of methane of each technique,
    - the cost of capture of carbon dioxide by each technique;
- to compare and select the optimal alternative amongst the three selected techniques (Absorption, adsorption and cold separation) based on criteria of yield and cost of gas capture thus obtained.

2 LITERATURE REVIEW

2.1 Overview of gas extraction at Lake Kivu

Lake Kivu is known to contain large amounts of carbon dioxide (CO_2) and methane (CH_4) in the deepest layers of water near the bottom surface[1]. Reserves are estimated at 60 billion Nm^3 of methane and 300 billion Nm^3 of carbon dioxide. The Lake reaches maximum depth of 480 m and gases are found dissolved from a depth of 260 m. Layers of water are stratified from more dense layers containing the dissolved gases below 260 m to less dense and gas-free layers from 260 m to the surface. Carbon dioxide originates from magma processes found in volcanic grounds under the Lake. Methane results from the reduction of carbon dioxide, which enters the bottom of the Lake, by deep water micro-organisms and from degradation of biological sediments settling from upper layers to the bottom of the Lake [1].

An independent expert committee issued a report in 2006 for a feasibility study for the Kibuye Stage 1 Power Limited (KP1) project [1]. The KP1project was a partnership between the Government of Rwanda and Dane Associates Limited for a pilot plant, then for a 35 MW power plant to be located at Kibuye, Rwanda. The purpose of the committee was primarily to recommend safe ways of extracting gas for the power plant while ensuring that the stability of various water layers above the bottom is still maintained. The committee indicated that substantial amount of methane continuously accumulates every year at the bottom of the Lake. The elevated hydrostatic pressure allows gases to dissolve and remain stable in solution. The concentration of dissolved gases was still below the saturation level in 2006. The natural rate of accumulation of methane has been estimated to 250 million Nm^3 per year and if no action is taken to degas the Lake, a catastrophic limnic eruption would result within the next 100 years due to saturation of the gases in deep water. The committee recommended therefore to extract gases from depth of 320 m or deeper. A minimum of three 35MW-power stations producing in total 105 MW was deemed enough to achieve the degassing rate of 250 million Nm^3 of methane per year.

A 25 MW power plant fueled by gas extracted from Lake Kivu was commissioned in 2015 at Kibuye by KivuWatt, a subsidiary of ContourGlobal [2]. The next phase of the process is to add a

generation capacity of 75 MW, which will total to about 110 MW, therefore exceeding the minimum rate of degassing recommended in 2006.

2.2 Methods for separation of binary mixture of carbon dioxide and methane

Both methane and carbon dioxide extracted from Lake Kivu are greenhouse gases. Their extraction process must therefore minimize venting to atmosphere as this undermines efforts to combat climate change. An extraction process at Lake Kivu should therefore recover high purity methane for power generation or for sale as natural gas, since methane is the main valuable product. High purity carbon dioxide will also be recovered and may be considered as a by-product gas from the Lake, which is then available for storage, sequestration or exportation for other uses.

The three commonly used methods to separate carbon dioxide are absorption in an alkaline solvent, cryogenic separation and adsorption on a membrane in industrial applications aimed at reducing greenhouse gas emissions [3].

2.3 Absorption of carbon dioxide in alkaline salt solutions

Zhang, Ye and Lu [4] have studied the vapor-liquid equilibrium behavior of aqueous solutions of potassium carbonate, bicarbonate and carbon dioxide. The effect of the concentration of potassium carbonate, the temperature of the solution and the initial load of carbon dioxide in solution on the total pressure and ratio of partial pressure of water to carbon dioxide was specifically investigated. It was found that when varying the concentration of potassium carbonate in the initial solution at high total pressure and high temperature, the ratio of the partial pressure of carbon dioxide to water at equilibrium was higher for solutions with a high initial concentration of potassium carbonate. Further increasing the temperature of the solution did not increase the partial pressure of carbon dioxide in the vapor phase. This result showed that when carbon dioxide is absorbed in a slurry with a high concentration of mixed potassium carbonate and bicarbonate, it may be recovered from that concentrated solution in a stripper operating at high pressure and high temperature and a much lower amount of evaporation of water from the solution would result. The vapor phase which leaves the stripper at high pressure contains a higher amount of carbon dioxide and little water, which can be removed by a condenser with a low duty. The carbon dioxide may then be

compressed for storage also with a lower duty of the compressor since already leaving the stripper at high pressure. The high concentration of the potassium carbonate in the solvent allows the stripper to operate with a lower duty of the reboiler to achieve high partial pressure of carbon dioxide in the overhead of the stripper. This results in total in less energy to desorb carbon dioxide from the solution and to compress it for storage compared to conventional absorption in monoethanolamine solutions. The overall absorption and stripping process were therefore considered as an alternative method which is less energy-intensive for capture of carbon dioxide from flue gas of power stations.

Jayaweera, Jayaweera, Elmore, Bao and Bhamidi [5] have discussed the use of mixed salt solutions to absorb CO_2 from post-combustion gas streams. Mixed solutions of ammonia and potassium carbonate at a bench scale and pilot scale experimental setup have been tested and were proven successful to remove CO_2 from flue gas at high loading in a flue gas from a coal-fired power plant. The process consists of a two-stage absorption step, first in an ammonia-rich solvent then in a potassium carbonate –rich solvent. The absorbed CO_2 was then stripped from the CO_2 rich solution in a second solvent regeneration. At the regeneration step, the ammonia-rich solution is recovered at the bottom of the column while the potassium carbonate-rich solution at an intermediate level on the column. The mixed salt absorption technology was found to provide the following benefits which outweighed the conventional neat ammonia, neat potassium carbonate or monoethanolamine processes: reduced emissions of ammonia and hazardous wastes, reduced cooling requirement since absorption occurs at low temperature with less heat of reaction produced, higher absorption rate, stable condition of salt in dissolved phase with no precipitation in solid form, lower duty of the reboiler at the solvent regeneration step and lower requirement of the energy to compress the pure CO_2 which is released from solution at high pressure in the regeneration column. The technology has been deemed economically feasible for post-combustion and pre-combustion CO_2 capture due to its reduced cost of 40$ per ton of CO_2 captured.

2.4 Cryogenic separation of carbon dioxide in natural gas recovery

In applications which involve separating water from methane during extraction of natural gas on offshore platforms, the priority in process design is to reduce the size and the weight of the separation equipment to install on the platform [6]. This is commonly achieved via cryogenic gas

separation as supersonic gas flows through a turbine. The natural gas at high pressure is accelerated through a turbine such that the temperature of the exhaust gas from the turbine drops below the freezing point of water at the lower outlet pressure of the turbine. Under such conditions, water is removed as dry ice from the natural gas. Hammera, Wahla, Anantharamana, Berstada and Lervåg [6] have conducted a simulation of a case to capture carbon dioxide in the form of dry ice for flue gases leaving a coal-fired power station by using a Laval nozzle (convergent-divergent nozzle) as the separation equipment. The Laval nozzle was selected since it is a small-size cold separation equipment with a lower footprint in comparison to supersonic turbines used on natural gas platforms to remove water from methane. The Peng-Robinson equation of state was used as the thermodynamic method of simulation in Hysys. The flowsheet was simulated to reduce the power consumption of the flue gas compressor upstream of the Laval nozzle. The duty of the feed compressor could be reduced with the Laval nozzle in comparison to the typical supersonic gas turbine used offshore in the Hysys simulation. The study concluded that the Laval nozzle could be used to separate carbon dioxide in dry ice form from the flue gas leaving the coal-fired power station by a small-sized process equipment with a similar energy-intensity than the conventional absorption in monoethanolamine. The benefit of this process is that it would require a lower capital investment than conventional absorption in monoethanolamine.

The aim of the study conducted by Mohamad [7] was to develop a mathematical model of the cryogenic process for separation of carbon dioxide from methane by desublimation or deposition of carbon dioxide in solid form on a packed bed at atmospheric pressure. Cryogenic separation of carbon dioxide from natural gas has been carried out at industrial scale by Exxon [7] during extraction of methane in gas deposits containing high concentration of carbon dioxide. The process of separation occurs in a cycle consisting of three phases: cooling of the bed, deposition of carbon dioxide onto the bed and regeneration of the bed. In the cooling phase, liquid nitrogen is passed through the bed and cools it to a cryogenic temperature below the deposition point of carbon dioxide (-78.5 °C) but still above the dew point of methane (-160°C) at atmospheric pressure. The next phase is the capture phase whereby carbon dioxide deposits in solid form on spherical particles which makes up the bed as its mixture with methane is passed through the cooled bed. The last phase is the bed regeneration phase whereby the deposited carbon dioxide

sublimates into a hotter gaseous stream of pure carbon dioxide passing through the bed. Water which deposited as ice during the capture phase also evaporates during the regeneration phase.

An experimental setup consisting of an insulated horizontal pipe filled with spherical marbles as particles forming the packed bed was designed to obtain characteristics of the bed such as the void fraction and the mean particle diameter, necessary to calculate heat and mass transfer coefficients in order to derive the profile of the deposition rate of carbon dioxide along the axial length of the packed bed. Simulations to close the material and energy balance across the packed bed for various molar concentrations of carbon dioxide in the gas mixture introduced in the packed bed were performed. These simulations demonstrated that a minimum space-time of 2 minutes was required to achieve a zero concentration of carbon dioxide in the gas at the outlet of the packed bed. Below 2 minutes, the contact time was not enough to completely deposit all the carbon dioxide contained in the gas at inlet of the bed. The optimal temperature range at atmospheric pressure was found to be between -80°C and -110°C for complete removal of carbon dioxide as solid deposited on the particles. The rate of deposition of carbon dioxide also increased with its molar concentration in the feed to the bed. Molar concentrations of up to 90% carbon dioxide in the feed led to high rate of separation from the mixture with methane. This revealed that cryogenic separation of carbon dioxide from methane was adequate for natural gas mixtures with a high concentration of carbon dioxide. A limited number of experiments were then conducted to verify the concentration profile obtained for a mixture of 70% CO_2 and 30% CH_4 fed from gas cylinders into the packed bed. The bed was previously cooled with liquid nitrogen at cryogenic conditions. The experiments demonstrated that carbon dioxide was completely removed at the outlet of the pipe but the actual concentration profile could not be verified due to constraints on installing many gas sample points along the axial length of the pipe used during the experiments as a plug flow reactor.

2.5 Adsorption of carbon dioxide on porous solids and membranes

Adsorption is also being considered as an alternative technique to capture carbon dioxide from gas mixtures due to its low energy requirements, its low capital cost and to the ease with which the adsorbent may regenerated by modulation of the pressure or temperature of the system to desorb the carbon dioxide after the adsorption step [8]. Hence three known types of adsorption are pressure wing adsorption (PSA), temperature swing adsorption (TSA) and vacuum pressure swing

adsorption (VPSA) depending on whether pressure or temperature is the variable modulated to regenerate the adsorbent. Though not yet available for post-combustion capture of CO_2 from flue gas due to the low capacity and selectivity of commercially available adsorbents, adsorption is considered for use in the separation of CO_2 from CH_4 in natural gas wells which are often not considered viable for exploitation during exploration of natural gas due the high content of carbon dioxide.

Abdullah, Idris, Shamsudin, Kim and Othman [8] conducted an experiment with the aim of selecting the best adsorbent for separation of CO_2 from a binary mixture with CH_4 at an initial concentration of 70% CO_2 by volume. Four adsorbents were considered in the study: Zeolite, which is crystalline aluminosilicates, Zirconium-benzene dicarboxylate, activated carbon made of material from a tropical hibiscus tree and activated carbon made from the shell of palm oil fruits. The four adsorbents were first analysed for three key characteristics which are mean pore size, particle size distribution and nitrogen adsorption capacity in cm^3 per gram of adsorbent under standard conditions of pressure and temperature. These key characteristics determine adsorption capacity. Activated carbon made from shell of palm oil fruit was found to be the best adsorbent with a pore size of about 20 Å, its nitrogen adsorption capacity was as high as 220 cm^3 per gram and its mean particle diameter 112μm. Tests were carried out with the four adsorbents at a pressure of 3 bar and at ambient temperature. Activated carbon made from the shell of palm oil fruit yielded superior affinity for carbon dioxide than methane: methane was recovered with a yield of 89% during adsorption at 3 bar and the purity of the carbon dioxide in the gas recovered during desorption at atmospheric pressure reached 94%.

He and Hägg [9] have evaluated the feasibility of different techniques to capture carbon dioxide based on energy consumption and cost of capture of carbon dioxide as criteria of comparison for fossil-fuel power stations. Energy consumption was quantified by thermal efficiency, i.e., the ratio of the net power exported by the power station including the carbon dioxide capture section to the heat generated by burning coal. Cost was defined as the investment cost of the process per unit amount of carbon dioxide captured. A baseline was defined for the net power output from the plant with the carbon capture section included. The most competitive technique would be the one which would achieve the baseline net power output of an existing plant without the carbon-capture facility at a higher thermal efficiency and lower cost of carbon capture. Two techniques were

investigated via simulations in HYSYS: adsorption on a fixed-site carrier membrane and conventional absorption in monoethanolamine. The results of the simulation achieved in terms of power consumption of auxiliary equipment such as compressors, pumps, expanders needed, were used to size process equipment relevant to each technique, therefore, to estimate utilities and capital cost for each case. Adsorption was found to have a higher thermal efficiency and a lower cost of capture than conventional absorption in monoethanolamine.

2.6 Economic evaluation criteria for preliminary technology selection

Sinnott [11], Peters and Timmerhaus[14] have discussed in detail various measures to assess the economic viability of an investment in a process or chemical plant by use of some reliable profitability measures. At an early stage during the design of a manufacturing process, alternative process flowsheets are normally obtained showing the sequence of major process equipment required to manufacture the finished chemical product or commodity. The calculations of the internal rate of return, also known as the discounted cash-flow rate of return is one of the simple methods to evaluate the economic performance of different options of flowsheet at an early stage of the project. At this point, only preliminary estimates of the cost of major equipment are available to the designer within an accuracy of ± 30%. This level of accuracy is enough to highlight design options that are worth further exploring in later stages of process design.

The internal rate of return takes into consideration the time-value of money over the entire life cycle of the project, thus offers a comprehensive to evaluate the profitability over the duration of the project which is the same for different alternative design routes being investigated. A simple definition of the internal rate of return is that it is the present-day interest rate which is just enough to ensure that the total capital invested in the present is paid back exactly at the end of the life cycle of the project. The internal rate of return is the value of r that satisfies the equation below over a time t, which is the life cycle of the process equipment before major renewal of the equipment is undertaken. For the purpose of this study, the depreciation of equipment over years of the project is excluded and the net annual profit is the difference between the gross annual income from sales of the commodity and the major annual cost of utilities required to achieve the desired separation between methane and carbon dioxide.

$$Total\ Capital\ Investment - \sum_{k=0}^{t} \frac{Net\ annual\ profit}{(1+r)^t} = 0$$

Recommended values of the internal rate of return in order to deem a preliminary flowsheet worth of further exploration span between 20 and 30%.

3 METHODOLOGY

The purpose of the research project is to compare three different potential techniques to separate carbon dioxide from methane during recovery of natural gas from Lake Kivu. This requires a definition of a rate of flow, common to the three techniques, at which the methane is to be produced during recovery via each given separation technique. This rate of flow serves as the basis for calculations to determine the size of equipment and the amount of utilities to be available for each technique. These latter quantities can then be used to obtain order-of-magnitude estimate of the capital and operating cost of each technique, hence enables comparison and selection of the cost-efficient amongst the three.

The study has been conducted following the four stages listed below.

3.1 Design basis and assumptions

5.1.1. Survey of data from Lake Kivu

Considering elements discussed in the preceding section, an estimated annual production rate of 250 million Nm^3 of methane is the degassing rate needed to maintain concentrations of dissolved gases at safe level in Lake Kivu. This comparative study will therefore be based on extracting high purity methane at a rate of 250 million Nm^3 per year at a depth of 320 m. The pressure at that depth is about 32 bar and the temperature 23°C. The dissolved gas concentrations at 320 m are 16 mmol/l of methane and 80 mmol/l of carbon dioxide [1].

5.1.2. Production rate

The annual volumetric flow rate required to degas Lake Kivu in order to maintain the concentration of dissolved toxic gases below safe level in its deep layers has been estimated as 250 million Nm3/year of methane at a purity of at least 98% (mol % or vol%). 98% methane is enough as a criterion to deem the recovered natural gas fit for commercialization in the world energy market [22].

5.1.3. Annual operating time and shutdown duration

The online time for the separation process is 330 days per year, hence the shutdown period for maintenance is 35 days per year. A storage of methane produced should be available to ensure that product is still delivered to the market during the 35 days per year when operation is posed for annual maintenance. To achieve an extraction rate of 250 million Nm^3/year of methane during 330 days of operation, the equivalent molar flow rate is about 391mol/s of 98% (mol %).

5.1.4. Material of construction

The presence of carbon dioxide dissolved in water implies that the presence of weakly acidic conditions in the streams of water extracted from the Lake. To ensure that the equipment to be installed for the methane recovery operation withstand the corrosive environment due to presence of dissolved carbon dioxide, stainless steel has been selected as material of construction for all equipment in this investigation.

3.2 Modelling in Aspen Plus V12 and sizing of process equipment

The objective of each separation technique to be investigated will be to recover 250 million Nm^3 per year of methane at 98% purity. 98% is considered as acceptable for export as natural gas. The volume (molar) composition of the gas mixture from Lake Kivu after extraction from the bottom consists mainly of 63% carbon dioxide, 36% methane and less than 1% of water vapor. At this stage, water has been separated from the gas. The initial temperature of the gas mixture fed to the separation equipment will be 20 °C and the starting pressure will vary according to each separation technique. This is the condition of the gas after having been extracted and separated from water at the surface obtained from an initial simulation in Aspen Plus V12.

The simulation in Aspen generates the preliminary size of major process equipment and the amount of utilities required for each of the three techniques being investigated.

3.2.1 Thermodynamic method

For each technique, an appropriate thermodynamic method to represent the behavior of carbon dioxide and methane mixture has been selected as recommended in Aspen Plus. Each technique has been simulated with the objective of achieving a final production rate of 250 million Nm^3 per

year of methane at 98% purity. The Soave-Redlich-Kwong (SRK) and the Peng Robinson cubic equation of state with the Boston-Mathias (PR-BM) alpha function cubic equations of state are used as property method in Aspen Plus for the flowsheets of cold separation and adsorption respectively. They are particularly recommended for gas processing, refinery and petrochemical applications.

For the case of the absorption flowsheet where carbonate and bicarbonate ions are present as ions in solution. The ENRTL-SR property method was selected in Aspen Plus V12. It is based on the Symmetric Electrolyte NRTL property model with the following considerations:

- the Redlich-Kwong equation of state for vapor phase properties
- the symmetric reference state (pure fused salts) for ionic species.
- Henry's law for solubility of supercritical gases.
- symmetric Electrolyte NRTL method of handling zwitterions

3.2.2 Selection of major process equipment

a. Piping for gas extraction

Carbon steel piping with a schedule 40 is selected for the piping to be submerged into the deep layers of the Lake in order to extract dissolved gases and route them to the surface. The maximum available diameter in the equipment cost estimator used is 0.508 m [15]. The length of the piping is taken as 320 m since this is the depth from which dissolved gas are extracted from the Lake.

The goal of the simulation in Aspen Plus V12 is to calculate the flow rate per piping with diameter of 0.508 m and length of 320 m required to achieve a gas phase emerging at the surface of the Lake with a molar content of 63 mol% carbon dioxide and 36 mol % methane. The starting liquid at a depth of 320 m has a composition of 8 mmol % carbon dioxide and 1.6 mmol% methane, the rest being Lake water. The piping is to ensure that the two-phase flow regime consists of gas bubbles dispersed in the liquid phase as the mixture is drawn upwards to the surface.

b. Gas-liquid separators or flash drums

Gas-liquid separators are required in the different sections of the flowsheets developed in this study to allow recovery of methane as the key profit component in the gas phase in which it emerges along with carbon dioxide after extraction from the Lake. Horizontal gas-liquid separators are sized by the Souders-Brown method [24] which is recommended as enough for preliminary sizing of gas-liquid separation vessels. Separation essentially occurs as liquids droplets flow vertically downwards, being removed from the bulk gas flow that occur upwards.

The liquids are considered to settle downwards under the influence of gravity as spherical droplets. A maximum allowable gas velocity is defined which must be less than or equal to the terminal settling velocity of the droplets from the gas phase. Should this gas velocity exceed the maximum, liquid droplets will be entrained upwards in the gas stream and separation will not take place. Therefore, the dimensions of the gas-liquid separator vessels are chosen to ensure that the gas velocity remains below the maximum allowable. The sizing equations used in this approach are therefore listed below.

The maximum allowable velocity of the gas in the separator is calculated by

$$v_{gas\ max} = K_s * \sqrt{\frac{(\rho_l - \rho_{g)}}{\rho_{g)}}} \qquad (1)$$

Where K_s is a sizing parameter given by $Ks = 0.152 * (L/3.05)^{0.56}$;
ρ_l is the liquid density in kg/m^3 and ρ_g is the gas density in kg/m^3.

The minimum vessel diameter to ensure that the maximum gas velocity is not exceeded is then calculated as

$$D_{min} = K_s * \sqrt{\frac{\frac{4}{\pi} * q_a}{v_{gas\ nax}}} \qquad (2)$$

where q_a is the gas flow rate at the actual flowing condition in m^3/s.
The available diameter of the vessel chosen is 4 m and the length-to-diameter is selected as 4. This implies that all gas-liquid separators are 4 m wide in diameter and 16 m long in length. The above

equation is then applied with material balance data from the simulation performed for each particular vessel in Aspen in order to calculate the minimum diameter, ensuring that it is less than 4 m, which is the standard size chosen for all vessels in this study.

c. Compressors

The duty of compressors is calculated in Aspen Plus V12 by specifying the required discharge pressure. Referring to Smith et al [12], it is assumed that isentropic compression takes place with both an isentropic and mechanical efficiency set at 70%.

d. Expansion valve

An expansion valve is required in the flow sheet of cold separation to enable the pressure drop required to generate the Joule-Thomson effect for cooling the gas below the boiling point of the mixture. At such low temperature, conditions are sufficiently cryogenic to achieve the removal of most of the CO_2 as liquid phase at the bottom of the gas-liquid separator drum. It is enough in Aspen Plus V12 to specify the pressure at the outlet of the pressure reduction valve.

e. Separation columns

Absorption and stripping columns

Packed beds are preferred in this study due to large liquid flow rates required for absorption into the liquid phase and desorption from the liquid phase of carbon dioxide [13]. The second reason for the choice of packed columns is the corrosive nature of solutions of carbonate or bi-carbonate ions present in the solution (alkaline media) where absorption or desorption of carbon dioxide takes place.

Table 1 Properties of Raschig rings packed columns

Properties of Raschig rings packed columns	
Aspen Plus V12	
Porosity	0.64
Particle diameter	13 mm
Bed spec surface, Sb	367.0/m
Available maximum column diameter	3 m
Column height	6 m

The choice of ceramic packing consisting of Raschig rings is therefore motivated by the above two considerations. Standard available columns with a maximum diameter of 3 m and a height of 6 m are selected [15]. The choice of the large diameter is motivated by the large flow rates through the packing, which allows moderate velocities of the gas and liquid phases contacting each other in the columns, thus low pressure drop across the packing. Low pressure drop is particularly necessary to ensure that the pressure in the columns remain high enough to minimize losses of water through evaporation, hence ensuring that concentrations of dissolved salts in the liquid phases are maintained below saturations levels. High evaporation of water from solutions could result into the precipitation of salts from solution and blockages in the process.

Adsorption and desorption columns

Some considerations have been noted while selecting adsorption as possible technique to separate methane from carbon dioxide in the gas extracted from Lake Kivu. For adsorption to be competitive to remove carbon dioxide and generate methane at high purity, activated carbon is to be used as the adsorbent. The choice of activated carbon is motivated by the fact that this commercial adsorbent has a high selectivity for carbon dioxide over methane. This is explained by an affinity for activated carbon to interact better with carbon dioxide than with methane as carbon dioxide is a more polar compound compared to the non-polar methane.

Abdullah et al [26]have conducted experiments to assess the performance of adsorption of carbon dioxide on activated carbon. Adsorption of carbon dioxide on activated carbon follows a type 1 isotherm, which is characteristic of monolayer absorption. According to this model, at constant temperature, the saturation concentration of CO_2 in the adsorbed phase increases with the partial pressure of CO_2 in the gas phase until a plateau is reached at higher pressures. The Freunlich equation has been found to provide a good model for the adsorption isotherm of CO_2 on activated carbon. The selectivity of carbon dioxide over methane on activated carbon has been recorded against pressure by Heuchel et al [25] at pressures of up to 15 bar, the selectivity value ranges between values of 1 and 10 at 5 bar.

Kinetics data on the adsorption of CO_2 at various pressures and temperatures on activated carbon have been reported by Singh and Kumar [27]. Results obtained were found to fit a pseudo second order kinetic model where the rate of adsorption of CO_2 is proportional to the square of free

adsorption sites available in the pores of the adsorbent. The free adsorption site available in the pores is expressed as the difference between the saturation concentration and the instantaneous concentration in the adsorbed phase.

Properties of beds of activated carbon have been sourced and derived from results obtained from the various sources. Those properties are reported in the table 2.

Table 2 Properties of packed bed of activated carbon

Properties of packed bed of activated carbon		
Hauchhum and Mahanta (2014)		
Porosity	0.5	
Bulk density	350	kg/m3
Particle diameter	0.92	Mm
Pore volume	0.068	cm3/g
Bed spec surface, Sb	543.0	/m
Total spec surface, S	1087.0	/m
Freunlich equation $C_{sat} = K * P_{CO2}^{\frac{1}{n}}$ where K = 0.505; n =1.701 at 5 bar, 298K C_{sat} , saturation concentration (mg CO2/g activated carbon) and P_{CO2}, partial pressure (bar)		
C_{sat} = 227.0 mg/g at 5 bar and 298 K		
Heuchel et al (1999)		
Selectivity range	1-10	
Singh and Kumar (2015)		
Rate of adsorption, $r_{CO2} = k * (M_{sat} - M)^2$ (mol/kg/s)		
k, CO2 adsorption rate constant (5 bar, 298K)	0.03 g AC/mg CO2/min 0.022 kg AC/mol CO2/s	
$M_{sat} = C_{sat}/44$ =227.0/44 = 5.15 mol/kg and M instantaneous concentration of CO2 in adsorbed phase in mol/kg		
	0.03	g/(mg.min)

The contact time between the gas and the adsorbent should also be long enough to enable enough adsorption of the carbon dioxide as the gas travels through the bed of adsorbent. This implies that the bed should be sized such that the superficial velocity of carbon dioxide is low enough to allow a longer contact time with the adsorbent. The adsorption step has slower kinetics and is the rate-limiting step as the gas passes through the adsorbent. To enable a low superficial velocity, the

diameter of the packed column containing the bed of activated carbon should be selected to be sufficiently large.

The low superficial velocity also enables to minimize pressure losses as the gas flows across the bed. The advantage of minimal pressure drop is that the operating pressure is maintained constant throughout the length of the bed and sufficiently high to enable adsorption at high rates throughout the bed. Adsorption occurs at faster rates as the operating pressure is increased.

As the gas extraction rate from the Lake will be large, in order to maintain the superficial velocity low enough through the adsorption bed, the gas flow will be split across many columns of identical diameter containing the same mass of adsorbent and arranged in parallel. In this manner, the flow rate through a single column is small enough to achieve a long contact time and an insignificant pressured drop.

As more carbon dioxide is adsorbed in each column, its bed of activated carbon becomes saturated with this compound and needs to be regenerated for the next cycle of adsorption. Each column will therefore undergo a cycle of adsorption and desorption. Desorption will be achieved by lowering the pressure in the column to vacuum conditions to allow carbon dioxide to return to the gas phase and free the bed of activated carbon for the next adsorption cycle, i.e., pressure swing adsorption. Each column undergoing an adsorption cycle will have a counterpart column undergoing the desorption cycle such that the production rate can be maintained by swinging each time between the saturated and the regenerated column.

f. Pumps

The power requirement for centrifugal pumps is calculated in Aspen Plus V12 by specifying the required discharge pressure. The overall efficiency of centrifugal pump is assumed as 75% (Smith, Van Ness and Abbott) [12],[23].

g. Heat exchangers

Shell-and-tube heat exchangers are chosen as the preferred standard type used in the process industries. The design with the floating head is recommended for the ease of maintenance of the

tube bundles that it provides [11]. Counter-current flow is the preferred arrangement used in all heat exchangers in the study.

The standard dimensions used for the tubes on all heat exchangers are outside diameter 0.019m; square pitch 0.0254m; tube length 4.88m and design pressure 690 kPa. Stainless steel is the material of construction of choice [15].

The sizing exercise consists of obtaining the duty of the heat transfer from the flowsheet model developed in Aspen. The log-mean temperature difference is then calculated for the counter-current flow arrangement. Given the typical ranges for values of the overall heat transfer coefficient reported by Sinnott [11] (Coulson and Richardson, volume 6), the area required for heat transfer is then calculated through the set of formula listed below.

The log-mean temperature difference is first calculated for the case of counter-current flow of material by

$$\Delta T_{LM} = \frac{(T_{hot\ in} - t_{cold\ out}) - (T_{hot\ out} - t_{cold\ in})}{ln(\frac{T_{hot\ in} - t_{cold\ out}}{T_{hot\ out} - t_{cold\ in}})} \qquad (3)$$

then the heat transfer area as

$$A = \frac{Q}{U * \Delta T_{LM}} \qquad (4)$$

quantities are ΔT_{LM} log-mean temperature difference (℃); $T_{hot\ in}$ the temperature of the hot stream entering the heat exchanger (℃); $T_{hot\ ou}$ the temperature of the hot stream leaving the heat exchanger (℃); $t_{cold\ in}$ the temperature of the cold stream entering the heat exchanger (℃); $t_{cold\ out}$ the temperature of the cold stream leaving the heat exchanger (℃); U the overall heat transfer coefficient (kW/m^2/℃); and A the required area in m^2.

Overall heat transfer coefficient relevant to this study are listed in table 3 [11].

Table 3 Overall heat transfer coefficient

Type of heat transfer	Hot stream	Cold stream	U (kW/m^2/℃)
Heater	Medium pressure steam at 150℃	Aqueous solution	1
Cooler	Gas	Cooling water at 19℃	0.3
Cooler	Aqueous solution	Cooling water at 19℃	0.8
Condenser	Aqueous vapor/condensing gas	Cooling water at 19℃	1
Vaporizer or reboiler	Medium pressure steam at 150℃	Aqueous solution	1.5
Exchanger 1	aqueous solution	aqueous solution	0.8
Exchanger 2	Gas	gas	0.01

3.3 Preliminary cost estimate

Table 4 Equipment costing equations [15]

Equipment	Size (S) Min - Max	Purchased Cost (C_p)	Constants in equation
Centrifugal compressor, motor-driven	75 – 6000 kW (power)	$C_p = a * S^b$	$a = 2193.2$; $b = 0.9435$
Centrifugal pump [23]	6 – 174 kW (power)	$C_p = a * \exp(b * S)$	$a = 8870.3$; $b = 0.0124$
Turbo-blower	1 – 4.72 m^3/s (flow)	$C_p = a * S^b$	$a = 45868$; $b = 0.616$
Expander, stainless steel gate valve, 1035 kPa rating	0.0508 – 0.305 m (diameter)	$C_p = a * S^2 + b * S + c$	$a = 139255$; $b = 8071.3$; $c = 1018.9$;
Shell-and-tube heat exchanger	9.3 – 1000 m^2 (area)	$C_p = a * S^2 + b * S + c$	$a = -0.04\ to\ -0.06$ $b = 234.41$; $c = 9000\ to\ 20\ 000$;
Absorption/stripping column, diameter 3m	6 – 50 m (height)	$C_p = a * S$+b	$a = 18291$ $b = 86158$
Ceramic packing for absorption/stripping columns diameter 3m	5.3 – 56 m (height)	$C_p = a * S$+b	$a = 5474$; $b = 3454$
Adsorption/desorption column, diameter 3m	1 – 20 m (height)	$C_p = a * S$+b	$a = 71317$ $b = -31.625$
Piping for degassing section	1 – 1 000 000 m (length)	$C_p = a * S$	$a = 128.5375$
Gas-liquid drum horizontal, diameter 4m, stainless steel, design pressure 1035 kPa [23]	7.9- 53.7 m (height)	$C_p = a * \mathrm{S} + \mathrm{b}$	$a = 12291$; $b = 50577$

A preliminary flowsheet has been obtained for each technique after simulation in Aspen Plus V12. The flowsheet reports the sequence of major pieces of process equipment, inlet and outlet process conditions as well as preliminary sizes of equipment. Bulk equipment sizes have been used to make preliminary estimates of the installed capital cost and of the cost of utilities for each technique of separation under this investigation.

The purchase cost of process equipment is estimated using the technique as recommended as described by Sinnott [11]; and Peters and Timmerhaus [14], [15]. The technique consists of first on inferring the unknown cost by scaling up the calculated size from the Aspen Plus models in relation to the size and cost of the same type of process equipment as known at a previous point in time.

Equations that approximate the online cost estimator of Peters and Timmerhaus (2002) are listed in table 4[15]. An equation is given for each type of equipment for a selected range of size or capacity. These are the equations used to estimate the purchased cost of each piece of equipment with the year 2002 as basis of reference for cost inflation.

The scaled-up cost of all equipment is then summed up to yield the total cost at the previous point in time. This previous total cost is then updated to current time by multiplying by a factor which is the ratio of the equipment cost index at present time to the same cost index at the previous point in time. The chemical plant cost index (CEPCI) published by the Chemical Engineering journal was used as the index for cost inflation over time in this research [15]. The total purchased cost is then multiplied by a cost installation factor in order to obtain the total installed cost of the equipment for each technique investigated.

Criteria for selection of utilities

a. Electricity

Electricity is available at a unit price of 0.095$/kWh in the local regions of the Democratic republic of Congo and Rwanda within the vicinity of Lake Kivu [18].

b. Steam

Medium pressure steam is supplied at 500 kPa and at a temperature of 150 ℃ [20].

c. Cooling water

Cooling water is essentially water taken from the Lake supplied to the process at a temperature of 19℃ [21].

4 DISCUSSION

4.1 Degassing section

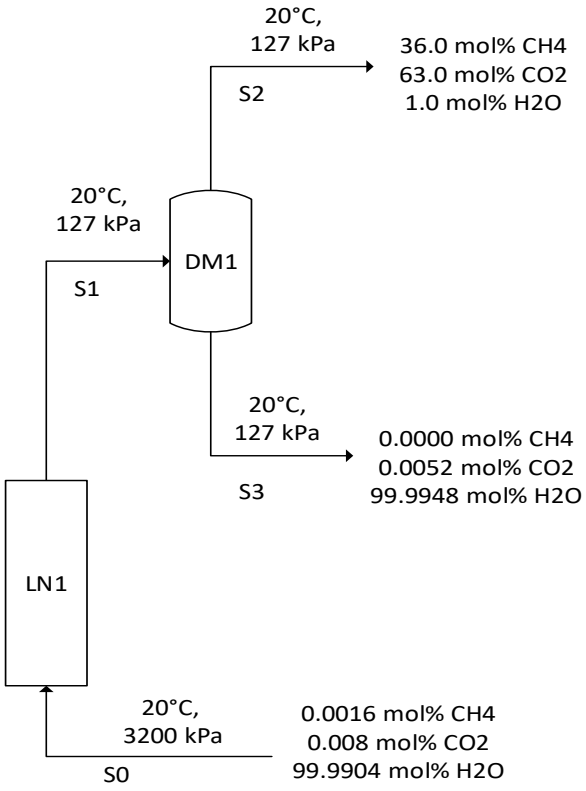

Figure 1Process flow diagram

Gas from the deep layers of the Lake is recovered in the degassing section. This is the first section of the plant, which is common to all three techniques of separation.

In the degassing section, water containing the dissolved gases rises from the bottom to the surface of the Lake through the piping system denoted LN1. This upwards flow is driven by the difference between the high pressure at the bottom of the Lake (3200 kPa) and the nearly atmospheric pressure at the surface (127 kPa). The flow happens at constant temperature of 20°C, which is the temperature in the deep layers of the Lake. As the pressure rises, gases emerged from the dissolved phase into the gas phase, hence the steam flowing up in the piping system LN1 consists of a gas-liquid flow. The piping system LN1 is submerged in the Lake. It emerges on the surface where it connects to the gas-liquid separator drums set DM1. During the degassing process, most of the

methane is recovered from the liquid into the gas phase as well as up to more than half of carbon dioxide. Most of the water containing the remaining amount of carbon dioxide is returned to the Lake at a higher elevation than the deeper layers of origin.

The calculated flow rate from the bottom of the Lake is 92 000 000 kmol/hr. This is the molar flow rate required to produce 250 million Nm^3 per year of methane, which is necessary to keep the concentration levels of dissolved gases below the safe level of 16 mmol/l of methane and 80 mmol/l of carbon dioxide.

The gas phase extracted in the degassing section contains about 36 mol% methane and 63 mol % carbon dioxide. This is the starting concentration for the next separation section where the purity of carbon dioxide is expected to be increased to at least 98 mol %. The molar flow rate of gas to be extracted in the degassing section depends on the separation efficiency of each of the three techniques to be explored in the next separation section.

Results of simulation in Aspen Plus V12 for the degassing section are presented in Appendix A – Aspen Plus V12 simulation results.

The vertical length of the submerged pipe from the bottom of the Lake to the surface is equal to 320 m, which is the average depth at which dissolved gases are present in water at the bottom of the Lake. A standard diameter for carbon steel piping available is 0.508 m15. For a single pipe with a diameter of 0.508 m and a vertical length of 320 m, the calculated flow rate to achieve process conditions was found to be 100 000 kmol/hr. This flow rate ensures that the flow regime in the pipe remains in a stable form where the emerging gas is dispersed as fine bubbles in

Table 5 Sizing of major pieces of process equipment (Appendices A and B)

Equipment	Type, size parameters per unit equipment	Quantity
Degassing piping, LN1	Carbon steel welded pipe, Sch 40 Available diameter: 0.508 m Flow per pipeline: 100 000 kmol/hr Total flow: 92 000 000 kmol/hr	920
Degassing drums, DM1	Type: horizontal tank Diameter: 4 m Length: 16 m Minimum diameter required: 3.1 m	1

the liquid phase. To achieve the total flow rate of 92 000 000 kmol/hr, the number of single pipes with diameter of 0.508 m is 920.

The purpose of the degassing section is only limited to siphon dissolved gases out of the liquid phases. This merely requires carbon steel piping which is submerged into the deep layers of the Lake from where water containing dissolved gases is extracted. Gases then emerge out of solution as the mixture flows upwards to the surface of the Lake.

Gas-liquid separators at the surface allow the gas phase to be removed as overhead while the liquid phase is routed back into the Lake. As such degassing only occurs via two-phase flow process and does not require utilities in the form of electricity, steam or cooling water.

Table 6 Purchased cost of major pieces of process equipment (Appendices A and B) [15]

Equipment	**Type**	**Cost per unit**	**Quantity**	**Subtotal**
Degassing piping, LN1	Carbon steel welded pipe, Sch 40 Available diameter: 0.508 m	$41 132	920	$37 841 440
Degassing drums, DM1	Type: horizontal tank Diameter: 4 m Length: 16 m	$247 233	1	$247 233
Subtotal (2002), CEPCI 390.4				$38 088 673
Subtotal (2022), CEPCI 877.5				$85 611 707

The total purchased cost of the degassing section is therefore limited only to the approximate capital cost of the pipeline and the gas liquid separators. This is the present-day capital cost reported as $85 611 707 in table 6. The cost to purchase piping represents the major portion of the capital investment for this section.

4.2 Absorption

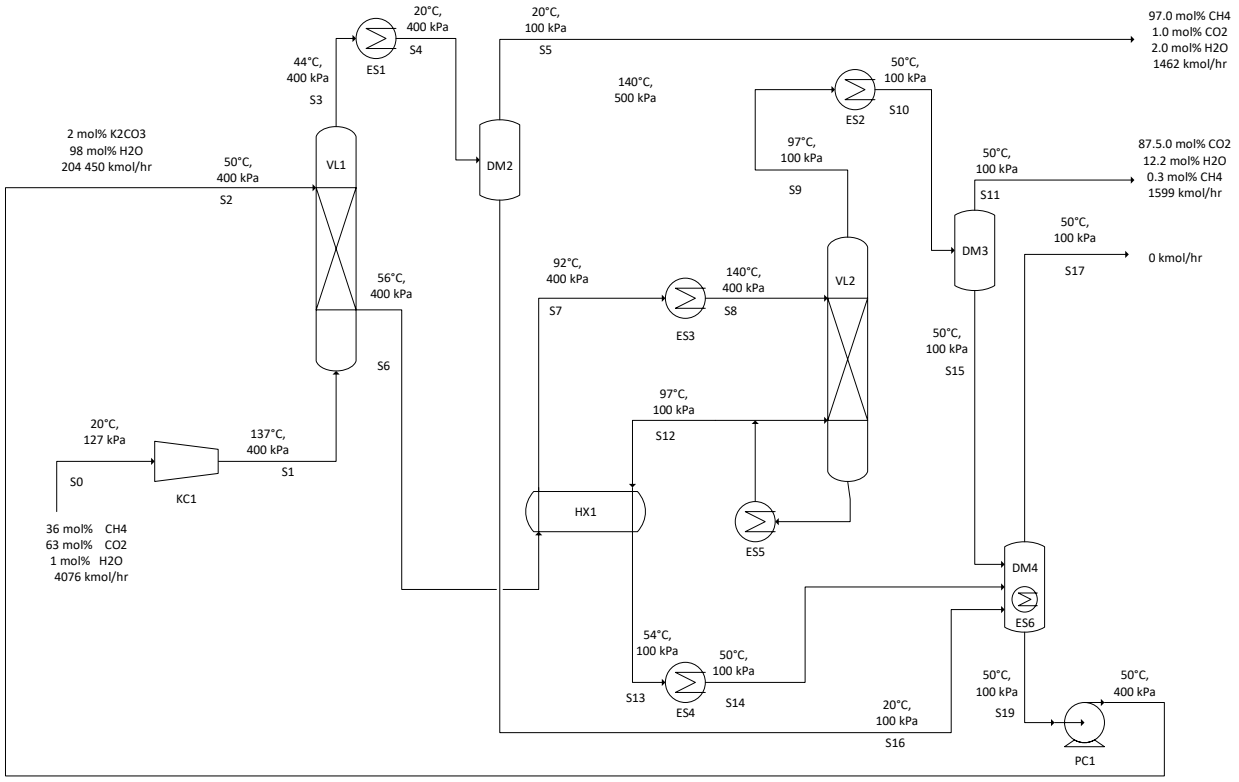

Figure 2 Process flow diagram

Gas from the degassing section received at 20°C is compressed by KC1 from 127 to 400 kPa. It then enters the absorption columns system VL1 at 137°C and 400 kPa. The absorption columns are packed columns where gas containing about 63 mol% carbon dioxide and 36 mol% methane is brought in contact with an alkaline solution of mixed potassium carbonate and potassium bicarbonate. Absorption of carbon dioxide takes place from the gas phase into the alkaline liquid phase through the equilibrium chemical reaction below where carbon dioxide is converted into the bicarbonate ion:

$$CO_{2(g)} + K2CO_{3\ (aq)} + H2O_{\ (l)} \leftrightarrow 2KHCO_{3\ (aq)}$$

Absorption takes place at a range of temperatures between 44 to 56°C at a pressure of 400 kPa. unreacted Methane passes through the columns and most of it exits in the overhead gas from the columns. This overhead gas is cooled in the water cooler ES1. Water that has evaporated from the column is condensed at outlet of ES1 and collected as liquid phase with some dissolved carbon

dioxide in the gas-liquid separator system DM2. The overhead gas from DM2 is the desired product methane recovered at 97 mol %.

The bicarbonate-rich solution leaving the absorption step flows through the heat integration heat exchangers HX1. Further heating is achieved through the steam heater ES3 at the outlet of which the bi-carbonate rich solution enters stripper columns system VL2. VL2 is fitted with the reboiler ES5. CO2 is stripped from the liquid phase at a pressure of 100 kPa and a range of temperature between 97 and 140 ℃, exits at the overhead of VL2 with mostly evaporated water. The overhead gas emerging from the stripping columns is cooled in ES2. Evaporated water from VL2 condenses at the outlet of ES2 and is recovered in the drums DM3, then in the mixing tank DM4. Emerging as gas phase from DM3 is a side stream containing at least 87 mol % CO2 with the balance being evaporated water.

The solution leaving at the outlet of the reboiler ES5 is mostly a lean solution of potassium bicarbonate. This lean solution is cooled in HX1, further in ES4 and collected in the gas-liquid separators DM4. In DM4, fitted with the heater ES6; condensed liquid from DM2 and DM3 systems are also collected in DM4. The solution in DM4 is bicarbonate-lean and is pumped back to the absorption section by PC1.

Separation by absorption produces natural gas containing 97% methane by mole (volume). The yield of this method for methane is close to 97%, meaning almost all the methane extracted from the Lake is recovered in the natural gas produced by this technique. The amount of methane lost with carbon dioxide is very little.

Results of simulation in Aspen Plus V12 for separation by absorption section are presented in Appendix A – Aspen Plus V12 simulation results. Sizing parameters for the absorption flowsheet are reported in table 7 below.

Table 7 Sizing of major pieces of process equipment (Appendices A and B) [15]

Equipment	Type, size parameters per unit equipment	Quantity
Feed compressors, KC1	Type: centrifugal motor driven Total load: 7 336 kW Available load per unit: 6 000 kW	2
Lean solvent to absorption columns pumps, PC1	Type: centrifugal motor driven Total load: 523 kW Available load per unit: 174 kW	3
Absorption columns, VL1	Type: packed column, stainless steel Height: 6 m Diameter: 3 m Packing type: Ceramic (Raschid) ring, 13 mm diameter, 6m high	1
Stripping columns, VL2	Type: packed column, stainless steel Height: 6 m Diameter: 3 m Packing type: Ceramic (Raschid) ring, 13 mm diameter, 6m high	1
Heat exchangers, rich solvents- lean solvent, HX1	Type: shell-and-tube, floating head, square pitch design Total duty: 130 000 kW Heat transfer coefficient: 0.8 kW/m^2/°C (Liquid-liquid) Mean-temperature difference: 5 °C Total area: 34 916 m^2 Available area per unit: 1 000 m^2	35
Absorption columns overhead gas condensers, ES1	Type: condenser, floating head, square pitch design Total duty: 655 kW Heat transfer coefficient: 0.3 kW/m^2/°C (gas/water) Mean-temperature difference: 8 °C Total area: 293 m^2 Available area per unit: 293 m^2	1
Stripping columns overhead gas condensers, ES2	Type: condenser, floating head, square pitch design Total duty: 656 647 kW Heat transfer coefficient: 1 kW/m^2/°C (aqueous vapor/water) Mean-temperature difference: 51 °C Total area: 12 892 m^2 Available area per unit: 1 000 m^2	13

Table 8 Sizing of major pieces of process equipment (Appendices A and B) [15]

Equipment	Type, size parameters	Quantity
Stripping columns feed heaters, ES3	Type: heater, floating head, square pitch design Total duty: 249 148 kW Heat transfer coefficient: 1 kW/m^2/°C (steam-aqueous liquid) Mean-temperature difference: 29 °C Total area: 8 742 m^2 Available area per unit: 1 000 m^2	9
Lean solvent from stripping columns coolers, ES4	Type: cooler, floating head, square pitch design Total duty: 25 908 kW Heat transfer coefficient: 0.8 kW/m^2/°C (water-water) Mean-temperature difference: 35 °C Total area: 929 m^2 Available area per unit: 929 m^2	1
Stripping columns reboilers in VL2	Type: vaporizer, floating head, square pitch design Total duty: 1 kW Heat transfer coefficient: 1.5 kW/m^2/°C (steam-aqueous solution) Mean-temperature difference: 53 °C Total area: 0.013 m^2 Available area per unit: 9.3 m^2	1
Mixing tank heaters in DM4	Type: heater, floating head, square pitch design Total duty: 50 kW Heat transfer coefficient: 1 kW/m^2/°C (steam-aqueous liquid) Mean-temperature difference: 100 °C Total area: 0.82 m^2 Available area per unit: 9.3 m^2	1
Gas-liquid separators, DM2	Type: horizontal tank Minimum diameter required: 1.0 m Diameter: 4 m Length: 16 m	1
Gas-liquid separators, DM3	Type: horizontal tank Minimum diameter required: 1.2 m Diameter: 4 m Length: 16 m	1
Mixing tank, DM4	Type: vertical storage tank Minimum diameter required: 7.5 m Diameter: 8 m Length: 16 m Volume: 804 m^3	1

The duty of the feed compressor KC1 has been calculated using efficiencies as discussed in Smith et al [12], it is assumed that isentropic compression takes place with both the isentropic and mechanical efficiency set at 70%. A pump is only required in the case of absorption used as a technique of separation. The overall efficiency of the centrifugal pump PC1 is assumed as 75% (Smith, Van Ness and Abbott) [12].

The RADFRAC packed absorption model was used in Aspen Plus V12 to estimate the required number of packed beds (number of equilibrium stages) for absorption of carbon dioxide into the alkaline solution in the first column VL1 and the stripping of the carbon dioxide from the alkaline solution in the second column VL2.

The duty of heat exchangers HX1, ES1, ES2, ES3, ES4, ES5 and ES6 are also reported in table 7. The log-mean temperature difference is then calculated for the counter-current flow arrangement. Given the typical ranges for values of the overall heat transfer coefficient reported by Sinnott [11] (Coulson and Richardson, volume 6), the area required for heat transfer is then calculated for each heat exchanger.

Horizontal gas-liquid separators DM1, DM2 and DM3 are sized by the Souders-Brown method[24]. Values for recommended length to diameter ratios and available diameters are from the online cost estimator for horizontal tanks [15],[24].

Table 9 Purchased cost of major pieces of process equipment (Appendices A and B) [15]

Equipment	Type	Cost per unit	Quantity	Subtotal
Feed compressors, KC1	centrifugal motor driven, 6 000 kW	$8 049 592	2	$16 099 184
Lean solvent to absorption columns pumps, PC1	centrifugal motor driven, 174 kW	$76 968	3	$230 904
Absorption columns, VL1	Packed column, D=3m; H = 6m	$195 904	1	$195 904
	Ceramic packing (porcelain, Raschid ring); D=3m; H = 6m	$36 298	1	$36 298
Stripping columns, VL2	Packed column, D=3m; H = 6m	$195 904	1	$195 904
	Ceramic packing (porcelain, Raschid ring); D=3m; H = 6m	$36 298	1	$36 298
Heat exchangers, rich solvents-lean solvent, HX1	Type: shell-and-tube, floating head, square pitch design, 1 000 m^2	$201 130	35	$7 039 550
Absorption columns overhead gas condensers, ES1	Type: condenser, floating head, square pitch design, 293 m^2	$80 470	1	$80 470
Stripping columns overhead gas condensers, ES2	Type: condenser, floating head, square pitch design, 1000 m^2	$201 130	13	$2 614 690
Stripping columns feed heaters, ES3	Type: heater, floating head, square pitch design, 1000 m^2	$201 130	9	$1 810 170
Lean solvent from stripping columns coolers, ES4	Type: cooler, floating head, square pitch design, 929 m^2	$187 254	1	$187 254

Table 10 Purchased cost of major pieces of process equipment (Appendices A and B) [15]

Equipment	**Type**	**Cost per unit**	**Quantity**	**Subtotal**
Stripping columns reboilers, ES5	Type: vaporizer, floating head, square pitch design, 9.3 m^2	$11 978	1	$11 978
Mixing tank heaters, ES6	Type: heater, floating head, square pitch design, 1000 m^2	$11 978	1	$11 978
Gas-liquid separator drums, DM2	Type: horizontal tank Diameter: 4 m Length: 16 m	$247 233	1	$247 233
Gas-liquid separator drums, DM3	Type: horizontal tank Diameter: 4 m Length: 16 m	$247 233	1	$247 233
Mixing tank, DM4	Type: vertical tank Diameter: 8 m Height: 16 m Volume: 804 m^3	$194 378	1	$194 378
Subtotal (2002), CEPCI 390.4				$29 085 490
Subtotal for Absorption section (2022), CEPCI 877.5				$65 375 301
Subtotal for Degassing section (2022), CEPCI 877.5				$85 611 707
Total purchase cost of major equipment				$150 987 008
Total capital investment (Lang Factor = 5.7 for Fluid processing plant)				$860 625 945

Table 11 Major annual cost of utilities (Appendices A and B) [15]

Utilities	Equipment & consumption	Annual consumption	Cost per unit	Subtotal
Electricity generated from local gas power plant	Compressors KC1 7 336 kW	58 101 120 kWh	0.095 $/kWh	$5 913 112
	Pumps PC1 523 kW	4 142 160 kWh		
Medium pressure steam, 4 bar and 150 °C, at current cost of energy from methane source [20]	Heaters ES3 249.148 MW	7 103 707 776 MJ	0.007 $/MJ [20]	$49 736 133
	Reboilers ES5 0.001 MW	28 512 MJ		
	Heaters ES6 0.050 MW	1 425 600 MJ		
Cooling water, mostly river water, 19°C [21]	Condensers ES1, 0.655 MW	18 675 360 MJ	0.000264 $/MJ [21]	$5 140 472
	Condensers ES2, 656.647 MW	18 722 319 264 MJ		
	Coolers ES4, 25.908 MW	738 688 896 MJ		
Total				$60 789 717

4.3 Adsorption

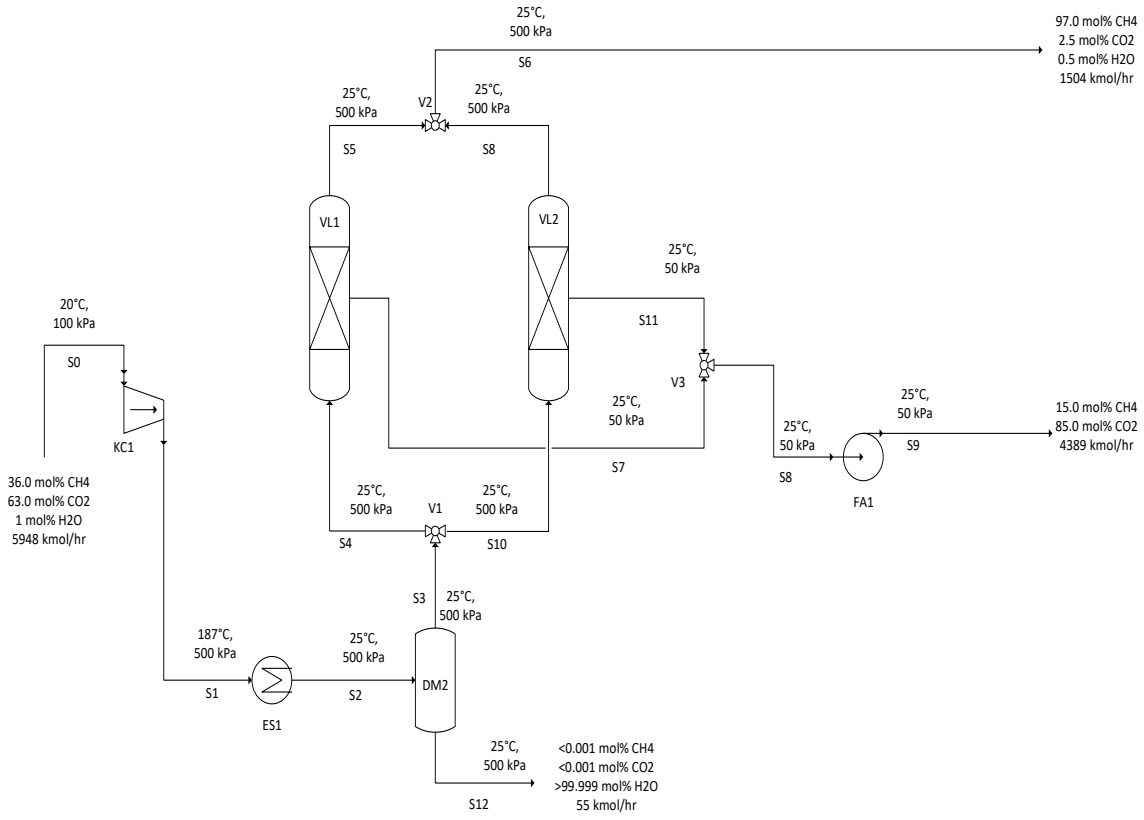

Figure 3 Process flow diagram

Gas from the degassing drums system DM1 is compressed to 500 kPa by the compression system KC1 then cooled in the water cooler ES1 to 25°C. Higher pressures and lower temperatures favor faster kinetics of adsorption and higher saturation concentrations of the adsorbed carbon dioxide in activated carbon. Condensate at the outlet of ES1 is removed in the set DM2 of gas-liquid separation drums. The overhead gas entering the adsorption columns consists of mostly 36 mol% CH_4 and 64 mol% CO_2.

The overhead gas is thus introduced at 25°C and 500 kPa in the set VL1 of packed adsorption columns that are online. The other set VL2 of packed adsorption columns are offline for regeneration of the adsorbent. The control valves V1, V2 and V3 are positioned such that gas the paths from DM2 to VL1 and at the outlet of VL1 to V2 are open to allow adsorption of CO_2; the paths from DM2 to VL2 and at the outlet of VL2 to V2 are closed; the path at the outlet of VL1 to

the blowers systems FA1 is closed while the path at the outlet of VL2 to the set of vacuum pumps FA1 is open to allow desorption of CO_2 from VL2.

Adsorption of CO_2 happens isothermally and nearly at constant pressure given the size of the packed columns that are selected so that pressure drop across the packing is minimized. At the same time some CH_4 is adsorbed although only in very small rates since the chosen operating conditions allow higher selectivity adsorption of CO_2 over CH_4 in activated carbon. At the outlet of the set of adsorption columns VL1, control valve V2 permits the flow of product containing 98 mol% CH_4 to exit the system. At 500 kPa and 25°C, the saturation concentration of CO_2 in activated carbon is reported as about 227 mg CO_2/g of adsorbent by Lalhmingsanga et al (2014). The breakthrough time is the time at which this concentration is reached. At the breakthrough time, the purity of methane will begin to drop below 95 mol % at the outlet of VL1. The set VL1 of adsorption columns will be switched offline to desorption mode while the set VL2 will be switched online to adsorption mode by swinging the positions of control valves V1, V2 and V3.

Desorption is done via pressure swing where the pressure in the saturated adsorption columns is reduced to 50 kPa or below via the suction of the blowers FA1. This low suction pressure created by FA1 allows most of the adsorbed CO_2 to return to the gas phase and be delivered at 85.0 mol% or higher.

Natural gas recovered via the adsorption technique also contains 97% methane by molar or volume fraction. However, adsorption has a low yield since only about 68% of methane in the gas extracted from the Lake is recovered in the natural gas produced from the Lake while a significant 32% of methane initially is lost in the by-product gas containing mostly carbon dioxide.

Table 12 Sizing of major pieces of process equipment (Appendices A and B) [15]

Equipment	Type, size parameters	Quantity
Feed compressors, KC1	Type: centrifugal, motor-driven Load: 15 774 kW Available load per unit: 6 000 kW	3
Feed coolers, ES1	Type: cooler, floating head, square pitch design Total duty: 11 646 kW Heat transfer coefficient: 0.3 kW/m^2/°C (gas-water) Mean-temperature difference: 49 °C Total area: 799 m^2 Available area per unit: 799 m^2	1
Gas-liquid separators, DM2	Type: horizontal tank Minimum diameter required: 1.5 m Diameter: 4 m Length: 16 m	1
Adsorption/desorption columns, VL1 and VL2	Type: packed column Height: 0.225 m Diameter: 3 m Mass of activated carbon: 5.6 ton	10
Blowers, FA1	Type: heavy-duty, centrifugal blower Volume flow rate: 217 066 m^3/hr Available volume flow rate: 16 992 m^3/hr	13

For the feed compressors KC1 and the blowers FA1, it is assumed again that an isentropic compression takes place with both the isentropic and mechanical efficiency set at 70% as discussed in Smith et al [12].

Properties of beds of activated carbon have been sourced from the work of Hauchhum et al; Heuchel et al [25]; Singh et al [27]. The simulation has produced the length of the packed bed of activated carbon reactor required to achieve adsorption of CO_2 so that the desired flow rate and purity of CH_4 is achieved at the outlet of the packed bed. This length is then used to estimate the mass and the cost of the adsorption beds in VL1 and VL2.

The log-mean temperature difference for the counter-current flow arrangement and the typical overall heat transfer coefficient reported by Sinnott [11] (Coulson and Richardson, volume 6) were used to estimate the area required for heat transfer for the feed coolers ES1.

Horizontal gas-liquid separators DM2 were also sized by the Souders-Brown method using the online cost estimator [15],[24].

Table 13 Purchased cost of major pieces of process equipment (Appendices A and B) [15]

Equipment	**Type**	**Cost per unit**	**Quantity**	**Subtotal**
Feed compressors, KC1	centrifugal motor driven, 6 000 kW	$8 049 592	3	$24 148 776
Feed coolers, ES1	Type: cooler, floating head, square pitch design, 799 m^2	$164 452	1	$164 452
Feed gas liquid-separator drums, DM2	Type: horizontal tank Diameter: 4 m Length: 16 m	$247 233	1	$247 233
Adsorption/desorption columns, VL1 and VL2	packed column	$16 014.7	10	$160 147
Blowers, FA1	Type: heavy-duty, centrifugal blower Available volume flow rate: 16 992 m^3/hr	$119 305	13	$1 550 965
Subtotal, CEPCI 390.4				$26 271 573
Subtotal, CEPCI 877.5				$59 050 475
Adsorbent (2022)[16], [17]	Activated carbon [16], [17]	$3 000/ton	5.6 ton	$16 800
Subtotal for Adsorption section (2022), CEPCI 877.5				$59 050 491
Subtotal for Degassing section (2022), CEPCI 877.5				$85 611 707
Total purchase cost of major equipment				$144 662 198
Total capital investment (Lang Factor = 5.7 for Fluid processing plant)				$824 574 529

Table 14 Major annual cost of utilities (Appendices A and B) [15]

Utilities	**Equipment & consumption**	**Annual consumption**	**Cost per unit**	**Subtotal**
Electricity generated from local gas power plant	Compressors KC1, 15 774 kW	124 930 080 kWh	0.095 $/kWh	$20 630 808
	Vacuum pumps FA1 11 646 kW	92 236 320 kWh		
Cooling water, mostly river water, 19°C	Coolers ES1, 11.646 MW	332 050 752 MJ	0.000264 $/MJ	$87 661
Total				$20 718 469

4.4 Cold separation

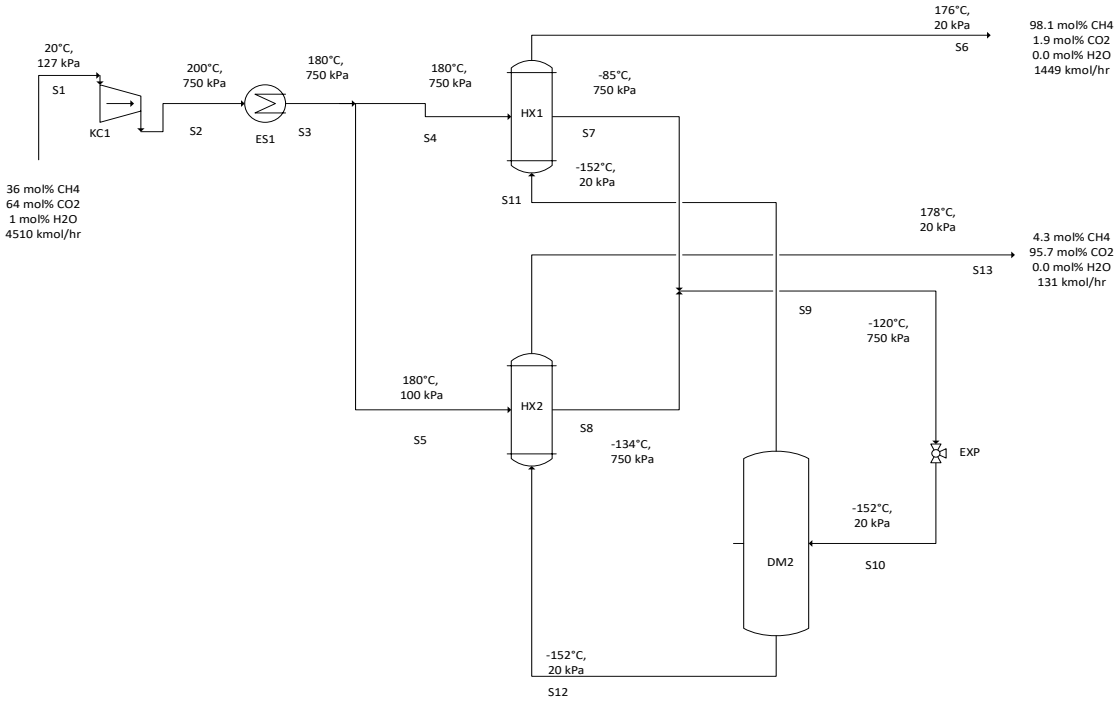

Figure 4 Process flow diagram

The driving factor for cold separation is the difference in boiling point or in volatility between CO_2 and CH_4 at low operating temperature. When a binary mixture of CO_2 and CH_4 is cooled, CO_2 being heavier than CH_4 is expected to condense first while most of the CH_4 to remain in the gas phase.

Gas from the overhead drums DM1 is compressed to 400 kPa. The compressed gas leaving the drums DM1 travels through a series of heat exchangers HX1, HX2, HX3 and HX4. These are a series of heat integration heat exchangers where hot gas leaving the compressor system KC1 at 130℃ is cooled to -102℃. The gas-liquid mixture leaving the cooling stage at -102℃ is collected in the system of separators DM2. Overhead gas from DM2 is further expanded from 400 kPa to a 100 kPa in the gas turbine system TB1. At the outlet of the turbine, a small portion of CO_2 and a trace of H_2O still in the gas phase is condensed and recovered as liquid in the separators DM3, heated up through the heat integration heat exchanger HX4, then the steam heater ES1 before being

recovered at nearly ambient conditions. The gas from DM3 is also heated up in the effluent-feed exchanger systems HX2, this gas leaving DM3 is the product CH_4 containing more than 98 mol%.

The condensed liquid from DM2 contains most of the CO_2 in the liquid phase, it is vaporized back in the effluent-feed exchanger HX3, expanded in the gas turbine systems TB2 and further passed in the heat exchanger HX1 to begin cooling the gas entering the compressors system KC1 from the cooling train. The product from HX1 is mostly carbon dioxide removed at more than 92 mol%.

Table 15 Sizing of major pieces of process equipment (Appendices A and B) [15]

Equipment	Type, size parameters per unit equipment	Quantity
Feed compressors, KC1	Type: centrifugal motor driven Total load: 11 788 kW Available load per unit: 6 000 kW	2
Heat exchanger, HX1	Type: shell-and-tube, floating head, square pitch design Total duty: 4 720 kW Heat transfer coefficient: 0.01 kW/m^2/°C (gas-gas) Mean-temperature difference: 22 °C Total area: 21 455 m^2 Available area per unit: 1 000 m^2	22
Heat exchanger, HX2	Type: shell-and-tube, floating head, square pitch design Total duty: 24 182 kW Heat transfer coefficient: 0.01 kW/m^2/°C (gas-gas) Mean-temperature difference: 25 °C Total area: 96 728 m^2 Available area per unit: 1 000 m^2	97
Cooler, ES1	Type: condenser, floating head, square pitch design Total duty: 1013 kW Heat transfer coefficient: 1 kW/m^2/°C (condensing gas - water) Mean-temperature difference: 171 °C Total area: 6 m^2 Available area per unit: 9.3 m^2	1
Expansion valve, EXP	Type: stainless steel gate valve Available diameter: 0.305 m	1
Degassing drums, DM2	Type: horizontal tank Diameter: 4 m Length: 16 m Minimum diameter required: 1.7 m	1

Utilizing cold separation, 88% of methane from the degassing section is recovered in the natural gas produced at a purity of 98% by mole or volume. About 12% is lost in the carbon dioxide by-product stream from the process.

Table 16 Purchased cost of major pieces of process equipment (Appendices A and B) [15]

Equipment	**Type**	**Cost per unit**	**Quantity**	**Subtotal**
Feed compressors, KC1	centrifugal motor driven, 6000 kW	$8 049 592	2	$16 099 184
Heat exchanger, HX1	exchanger, floating head, square pitch design, 1000 m^2	$201 130	22	$4 424 860
Heat exchanger, HX2	exchanger, floating head, square pitch design, 1000 m^2	$201 130	97	$19 509 610
Cooler, ES1	Type: vaporizer, floating head, square pitch design, 9.3 m^2	$11 978	1	$11 978
Expansion valve, EXP	Type: stainless steel gate valve Available diameter: 0.305 m	$16 435	1	$16 435
Degassing drum, DM2	Type: horizontal tank Diameter: 4 m Length: 16 m	$247 233	1	$247 233
Subtotal (2002), CEPCI 390.4				$40 371 352
Subtotal for Cold separation (2022), CEPCI 877.5				$90 742 473
Subtotal for Degassing section (2022), CEPCI 877.5				$85 611 707
Total purchase cost of major equipment				$176,354,180
Total capital investment (Lang Factor = 5.7 for Fluid processing plant)				$1 005 218 826

Table 17 Major annual cost of utilities (Appendices A and B) [15]

Utilities	**Equipment & consumption**	**Annual consumption**	**Cost per unit**	**Subtotal**
Electricity generated from local gas power plant	Compressors KC1 11 788 kW	93 360 960 kWh	0.095 $/kWh	$8 869 291
Cooling water, mostly river water, 19℃	Coolers ES1, 1.013 MW	28 882 656 MJ	0.000264 $/MJ	$7 625
Total				$8 876 916

4.5 Benefits of the three separation techniques

Two important benefits have been defined as part of initiatives for the degassing of Lake Kivu. The first goal to achieve is to extract toxic dissolved gases that accumulate in the deep layers of the Lake, hence enable their concentration to remain below levels safe enough to prevent the ecological devastation that could result on the surface should a natural volcanic eruption of high magnitude occurs in the region. The second goal is to separate methane from carbon dioxide as the methane accumulating in the deep layers of the Lake is a useful energy source for the generation of electricity than can be sold or exported to both local east African markets surrounding the Lake and much larger world markets than the east African great Lakes region.

The first goal ensures environment safety for the region in case of a natural disaster impacting the stability of dissolved layers of gases in the Lake and does not necessarily pursue a direct economic benefit to result for the capital invested. The second goal builds on the opportunity of supplying energy to markets by beneficiation of the natural gas that accumulates through natural processes in the Lake. As electricity is generated and sold from this natural gas, financial income then results. An analysis is then possible to identify the economic worth of each of the three techniques explored in this study. By comparing the income generated by the local sale of electricity produced from the methane recovered via each of the three techniques to the respective cost of the capital, the three methods can be ranked according to a suitable measure of profitability by this preliminary study. This ranking then allows to select the technique with the most favorable measure of financial viability for further detailed engineering and appraisal.

The measure of profitability to be used in this study estimate is the internal rate of return or discounted rate of return on the cash flow or net income from the generation of electricity from methane. The basis for this evaluation is reported in the table. The price of energy from methane is taken as 0.095$/ kWh18 as is currently in the local markets surrounding the region (DRC and Rwanda). The expected service life of the installation to recover methane is taken as 14 years as recommended by Peters and Timmerhaus[14] for the case of a natural gas production site. The annual operating time is 330 days. The minimum Wobbe Index of methane is reported as 11 452 kCal/Nm3 and converted to 13.319 kWh/Nm3 of gas [28].

Table 18 Economic parameters for profitability analysis

Typical service life (Natural gas production plant)	14 years
Annual operating time	330 days
Lower Wobbe index of methane	11 452 kCal/Nm^3 or 13.319 kWh/ Nm^3
Price of electricity, Lake Kivu areas (2022)	0.095$/ kWh
Gross unit income	1.30 $/ Nm^3

The unit gross income from the sale of electricity is calculated as 1.30 $/Nm3 of methane produced. This unit income is common to all three techniques explored in this study.

4.6 Comparison of yield and natural gas product purity

All three techniques of separation have the potential to generate natural gas at more than 75 mol % of methane, which is the minimum recommended purity for commercial natural gas. The condition to generate at least 250 million Nm^3/year of natural gas is also satisfied by all three techniques of separation.

Table 19 Yield and product purity

Method of separation	Methane purity (mole or volume %)	Yield (%)
Absorption	97	97
Adsorption	97	68
Cold separation	98	88

The purity and the yield of methane achieved is not identical for all three cases. While cold separation allows to achieve the highest purity of 98 mol%, 97 mol % can be attained with both absorption and adsorption methods. Absorption in potassium bicarbonate has the highest yield of 97% followed by cold separation with 88% and adsorption figures last with only 68%.

4.7 Comparison of gross income from sales of electricity

Table 20 Gross annual income

Minimum annual methane production rate (million Nm^3)	Unit gross income ($/$Nm^3$)	Annual gross income (million $)
250	1.30	325

The minimum production requirement was defined as 250 million Nm^3/year. This would yield 325 million $ worth of gross income from sales of electricity at the current price of about 0.095 $/ kWh[18]. This requirement is common to all three techniques.

4.8 Comparison based on total capital investment

The techniques are evaluated by comparing their specific cost of capital to purchase the equipment and their specific cost of utilities. For each technique the total cost of the equipment includes the cost of the degassing section situated upstream of the actual section where separation between carbon dioxide and methane is realized. Results obtained are presented in the table below.

Table 21 Total Capital investment (Appendix B)

Method of separation	Total capital investment
Absorption	$860 625 945
Adsorption	$824 574 529
Cold separation	$1 005 218 826

Cold separation is the most expensive technique based on cost of capital needed to purchase the equipment. The cost of heat exchangers required in the heat integration scheme that creates cryogenic conditions necessary to achieve the separation of gases is the primary drive of this capital cost followed by the cost of compression of the gas received from the degassing section located upstream.

Absorption is ranked second in terms of the cost of the required capital investment. Absorption also has a large footprint as it requires many pieces of equipment in order to achieve the desired

separation of gases. With this technique, compressors needed to increase the pressure of gas to higher values which enhance the rate of transfer of carbon dioxide in the alkaline solution of potassium carbonate represents the major contributor to the cost of the equipment to purchase. Adsorption in activated carbon requires the least total capital investment in order to recover natural gas from Lake Kivu. The cost of the compressors that are required to deliver the higher operating pressure at which the higher saturation concentration of carbon dioxide in activated carbon can be achieved represents the major portion in the capital investment when this technique is employed.

4.9 Comparison based on net annual income

Based on results listed in the table above, absorption is the most expensive to operate, followed by adsorption and cold separation.

Table 22 Annual operating cost (Appendix B)

Method of separation	Major annual cost of utilities
Absorption	$60 789 717
Adsorption	$20 718 469
Cold separation	$8 876 916

The common cost contributor in adsorption and cold separation is that of compression that is required at the beginning of the separation steps when these two methods are to be employed. Absorption stands out as the most expensive technique due to the cost of medium pressure steam required when this method is selected. Medium pressure steam is required to raise the temperature of the solution rich in potassium carbonate leaving the absorption step as it enters the stripping section. This is the step where carbon dioxide is removed in the gas phase, leaving a solution which is lean in carbonate in order that can be recycled to the preceding absorption step.

Table 23 Net annual income (Appendix B)

Method of separation	Net annual income
Absorption	$264 210 283
Adsorption	$304 281 531
Cold separation	$316 123 084

When the cost of utilities, taken as the major operating cost of the given separation technique is subtracted from the gross income of 325 million $, the calculated net annual income result is reported above for each technique of separation. It is then noticed that cold separation is more favorable in terms of net annual income, followed by adsorption and absorption figures as the least favorable candidate amongst the three methods.

4.10 Comparison based on internal rate of return

Results of the total capital investment of section 7.4 and of the net income of section 7.5 are later combined to calculate the internal rate of return for the three cases. The useful service lifetime is defined as 14 years for a natural gas production plant.

Table 24 Internal rate of return (refer to Appendix C)

Method of separation	Internal rate of return
Absorption	30%
Adsorption	36%
Cold separation	31%

In summary, adsorption in activated carbon finally appears as the most viable separation technique with an internal rate of return of 36%. This figure indicates that the method is enough to guarantee higher return on investment over the entire lifetime of the natural gas production operations at Lake Kivu during separation carbon dioxide from methane.

Results in table x are obtained by an approach that is simple but enough for a study estimate. This approach allows to single out the most cost-efficient route between the three selected techniques.

Cold separation and absorption almost have an equal internal rate of return near 30%. An initial decision choosing cold separation would have to be motivated by the availability of a large amount of capital to cover for the total cost of expensive equipment and if absorption was selected, an initial low cost of energy to generate steam required in this technique would be the supporting factor.

Nevertheless, for the purpose of this study estimate, adsorption in activated carbon is selected and worth to be investigated for detailed analysis in the subsequent steps of the appraisal process of the Lake Kivu natural gas recovery initiatives.

5 CONCLUSION AND RECOMMENDATIONS

Carbon dioxide occurs along with methane in solution at elevated depth in the Lake. The concentration of these gases is monitored, and recent measurements have demonstrated their continuous accumulation in the deep layers of the Lake. Beyond a threshold of concentration, these gases may emerge from solution and cause devastation to the eco-systems surrounding the Lake. The risk posed by the accumulation of these gases in the Lake can be properly mitigated by degassing the Lake to maintain their concentration below safety limits. A minimum degassing rate to achieve is defined as 250 million Nm^3 of methane recovered per year.

Methane and carbon dioxide can therefore be recovered by degassing the Lake. Methane offers the additional advantage of being an energy source for the subsequent generation of electricity. An opportunity therefore arises to recover methane from carbon dioxide once these gases are extracted from the Lake. An investigation into three different techniques to separate methane and carbon dioxide for the case of the extraction of dissolved gases from Lake Kivu has been conducted in this study.

Preliminary process flowsheets were developed listing the major pieces of process equipment with their approximate sizes. These are the preliminary designs required to achieve the recovery of methane from a gas mixture with carbon dioxide via each of the three techniques. The total capital investment and the annual cost of major utilities were further calculated for the three techniques in the form of study estimates. These estimates were further processed into a basic profitability analysis to assess the most economically viable route by use of the internal rate of return as the financial criterion of selection between the three methods of gas separation.

Absorption has been found to yield the smallest internal rate of return, hence ranked the less favorable route to employ for this type of separation. The absorption flowsheet is characterized by a moderate cost of the capital for the process equipment but by a steep annual cost of operation. The inflated cost of operation with this method is due to the large consumption of steam which is required as energy source to supply heat required to generate the alkaline solution in which carbon dioxide is dissolved leaving a pure stream of methane as product [31].

Cold separation yields the largest costs of capital for the process equipment and the lowest annual operating cost. The cost of compressors required in this flowsheet represents the major contributor to the capital investment. This method is then ranked as the middle choice in terms of the internal rate of return. It allows methane to be recovered as a much purer gas while most of the carbon dioxide is knocked out as liquid phase at very cold temperature.

Adsorption in activated carbon is finally selected as the most favorable technique to achieve the recovery of methane from carbon dioxide for its highest internal rate of return. The drawback of this method is its low yield since a significant amount of methane is also adsorbed along with carbon dioxide in activated carbon. Results of simulations in Aspen Plus prove, as discussed by Abdullah et al (2019), that adsorption is the most cost-competitive amongst the three techniques when recovering methane from reservoir formations with a high content of carbon dioxide due to its lower energy consumption and smaller plant equipment footprint [8].

In spite of the lowest yield, adsorption affords the benefits of the smallest cost of the capital investment to purchase process equipment and of moderate annual cost of electricity to drive compressors needed for the adsorption step and vacuum blowers for the desorption step where activated carbon is regenerated for the next cycle of adsorption and desorption. These economic advantages offered by the technique of adsorption in activated carbon are enough to offset the concern of the low yield of methane.

In light of the preceding discussion on the outcome of simulations conducted in Aspen, a few recommendations can be made to validate and further substantiate the findings of this research.

- Results obtained in this study are only preliminary estimates with an accuracy of ± 30% but obtained with enough truthfulness to recommend the use of adsorption as the preferred technique of gas separation.
- The accuracy of these estimates may be further improved by more rigorous method of sizing and costing process equipment for the adsorption process flowsheet developed in this study.

- The adsorption of carbon dioxide in activated carbon was modelled in Aspen Plus V12 as pseudo second-order chemical reaction in a plug-flow reactor model. Experimental kinetic data that match the actual the adsorption process was entered in the plug flow reactor model in Aspen. In this model, carbon dioxide and methane in the adsorbed phase were represented as pseudo-solids components. A recommendation to validate this modelling approach is to use the Aspen Adsorption software which is deployed as a distinct software in the Aspen Plus V12 package as method of verifying results obtained in this study when sizing the adsorption and desorption columns.
- Experimental studies are further to be designed in order to test the actual degassing of samples of water from Lake Kivu. The resulting gasses must then be processed into activated carbon to practically assess the effectiveness of adsorption as suitable technique of separation.
- Carbon dioxide and methane are both greenhouse gases. Apart from extracting then from the Lake to prevent the aftermath of a catastrophic eruption from the Lake, a responsible approach is to store the concentrated stream of carbon dioxide to other safe locations. Technologies involving capture, sequestration or use of the carbon dioxide that will further result after energy is produced from methane should further be investigated. These technologies will ensure that carbon dioxide is not merely released into the atmosphere after having been removed from Lake Kivu.
- The region of the east African Great Lake is also certified to contain large reserves of unexploited hydrocarbons. A recommendation is to consider the re-use of the carbon dioxide that is produced at Lake Kivu for enhanced recovery of crude oil from nearby reservoirs of hydrocarbons. These reservoirs could provide safe sinks where to store the carbon dioxide recovered from operations at Lake Kivu.

REFERENCES

[1]. Kling G, MacIntyre S, Steenfelt JS, Hirslund F. Lake Kivu Gas Extraction. Report on Lake Stability. Report no. 62721-0001, Issue no.0. Independent Expert Committee, July 12, 2006; Santa Barbara (US).

[2]. Power Technology [Internet]. KivuWatt Project, Lake Kivu, Kibuye, Available from https://www.power-technology.com/projects/kivuwatt-project-Lake-kivu-kibuye/

[3]. CO2 Capture Project [Internet]. Three basic methods to separate gasses. Available from https://www.co2captureproject.org/pdfs/3_basic_methods_gas_separation.pdf

[4]. Zhang S., Ye X., Lu Y. Development of a Potassium Carbonate-Based Absorption Process with Crystallization-Enabled High-Pressure Stripping for CO2 Capture: Vapor–Liquid Equilibrium Behavior and CO2 Stripping Performance of Carbonate/Bicarbonate Aqueous Systems. ScienceDirect 2014, Energy Procedia (63); 665 – 675.

[5]. Jayaweera I, Jayaweera P, Elmore R, Bao J, Bhamidi S. Update on mixed-salt technology development for CO2 capture from post-combustion power stations. ScienceDirect 2014, Energy Procedia (63); 640-650.

[6]. Hammera M, Wahla PE, Anantharamana R, Berstada D, Lervåg KY. CO2 capture from offshore gas turbines using supersonic gas separation. ScienceDirect 2014, Energy Procedia (63); 243-252.

[7]. Mohamad NSB. CRYOGENIC SEPARATION OF C02 FROM METHANE. (BEng (Hons), dissertation). Universiti Teknologi PETRONAS, Department of Chemical Engineering; May 2012; Malaysia.

[8]. Abdullah A, Idris I, Shamsudin IK, Kim J, Othman MR. Carbon Dioxide Separation form Carbon Dioxide-Methane Gas Mixture Using PSA Utilising Inorganic and Organic Adsorbents. 6th International Conference on Environment (ICENV) 2018, School of Chemical Engineering, Universiti Sains Malaysia, Penang, Malaysia.

[9]. He X, Hägg MB. Energy Efficient Process for CO2 Capture from Flue gas with Novel Fixed-site-carrier Membranes. ScienceDirect 2014; Energy Procedia (63); 174-185.

[10]. Jansen D, Ramirez A. Performance requirements for CO2 capture technologies; How realistic are capture cost targets? ScienceDirect 2014; Energy Procedia (63); 45-52.

[11]. Sinnott RK, Chemical Engineering Design; Chemical Engineering, volume 6, 4th Edition 2005; Coulson & Richardson's Chemical Engineering Series.

[12]. Smith JM, Van Ness HC, Abbott MM. Introduction to Chemical Engineering Thermodynamics, 6th Edition 2001.

[13]. Seider WD, Seader JD, Lewin DR. Product & Process Design Principles. Synthesis, Analysis and Evaluation, 2nd Edition 2004.

[14]. Peters MS, Timmerhaus KD, Plant Design and Economics for Chemical Engineers, 4th Edition 1991.

[15]. Equipment Costs calculator, Plant Design and Economics for Chemical Engineers, 5th Edition, Available from http://www.mhhe.com/engcs/chemical/peters/data/ (Accessed on 3/12/2022)

[16]. Activated Carbon Price Trend, Available from https://www.procurementresource.com/resource-center/activated-carbon-price-trends (Accessed on 3/12/2022)

[17]. U.S. – Activated Carbon- Market Analysis, Forecast, Size, Trends And Insights Update: COVID-19 Impact, Available from https://www.indexbox.io/blog/activated-carbon-price-per-ton-june-2022/ (Accessed on 3/12/2022)

[18]. Democratic Republic of the Congo electricity prices, Available from https://www.globalpetrolprices.com/Democratic-Republic-of-the-Congo/electricity_prices/ (Accessed on 3/12/2022)

[19]. Natural Gas Price, Available from https://www.oilcrudeprice.com/natural-gas-price/ (Accessed on 3/12/2022)

[20]. TLV. A Steam Specialist Company, Available from https://www.tlv.com/global/US/calculator/steam-unit-cost.html (Accessed on 3/12/2022)

[21]. Big Chemical Encyclopaedia, Available from https://chempedia.info/info/cooling_water_costs/ (Accessed on 3/12/2022)

[22]. Natural Gas Composition and Specifications, Available from https://www.e-education.psu.edu/fsc432/content/natural-gas-composition-and-specifications (Accessed on 3/12/2022)

[23]. Calculation of Pump Efficiency: Formula & Equation, Available from https://www.linquip.com/blog/pump-efficiency/ (Accessed on 3/12/2022)

[24]. Gas-Liquid Separators Sizing Parameter, Available from http://www.jmcampbell.com/tip-of-the-month/2015/09/gas-liquid-separators-sizing-parameter/#:~:text=There%20are%20two%20methods%20for%20sizing%20gas-liquid%20separators%3A,has%20shortcomings%20in%20terms%20of%20quantifying%20separator%20performance. (Accessed on 3/12/2022)

[25]. Heuchel M, Davies GM, Buss E, Seaton NA. Adsorption of Carbon Dioxide and Methane and Their Mixtures on an Activated Carbon: Simulation and Experiment. Langmuir 1999, 15, 8695-8705.

[26]. Abdulah A, Idris I, Shamsudin IK et al. Carbon dioxide separation from carbon dioxide-methane gas mixture using PSA utilizing inorganic and organic adsorbents 2019; AIP Conference Proceedings 2124, 020058.

[27]. Singh VK, Kumar EA. Comparative Studies on CO_2 Adsorption Kinetics by Solid Adsorbents. Science Direct 2016; Energy Procedia (90) 316 – 325.

[28]. The Engineering Toolbox. Fuel Gases - Wobbe Index. Available from

[29]. https://www.engineeringtoolbox.com/wobbe-index-d_421.html (Accessed on 3/12/2022)

[30]. Fowkes ND, Mason DP, Hutchinson AJ. Gas emissions from Lake Kivu. Environmental Science, 2018.

[31]. Badiei M, Asim N, Yarmo M A, Jahim JMd1, Sopian K. Overview of Carbon dioxide Separation Technology. Proceedings of the IA STED International Conference Power and Energy Systems and Applications (PESA), 2012.

[32]. Damen K, van Troost M, Faaij A, Turkenburg W. A comparison of electricity and hydrogen production systems with CO2 capture and storage. Part A: Review and selection of promising conversion and capture technologies. Progress in Energy and Combustion Science 32 215–246, Science Direct 2006.

Appendix A – Aspen Plus V12 simulation results

A.1. Degassing section

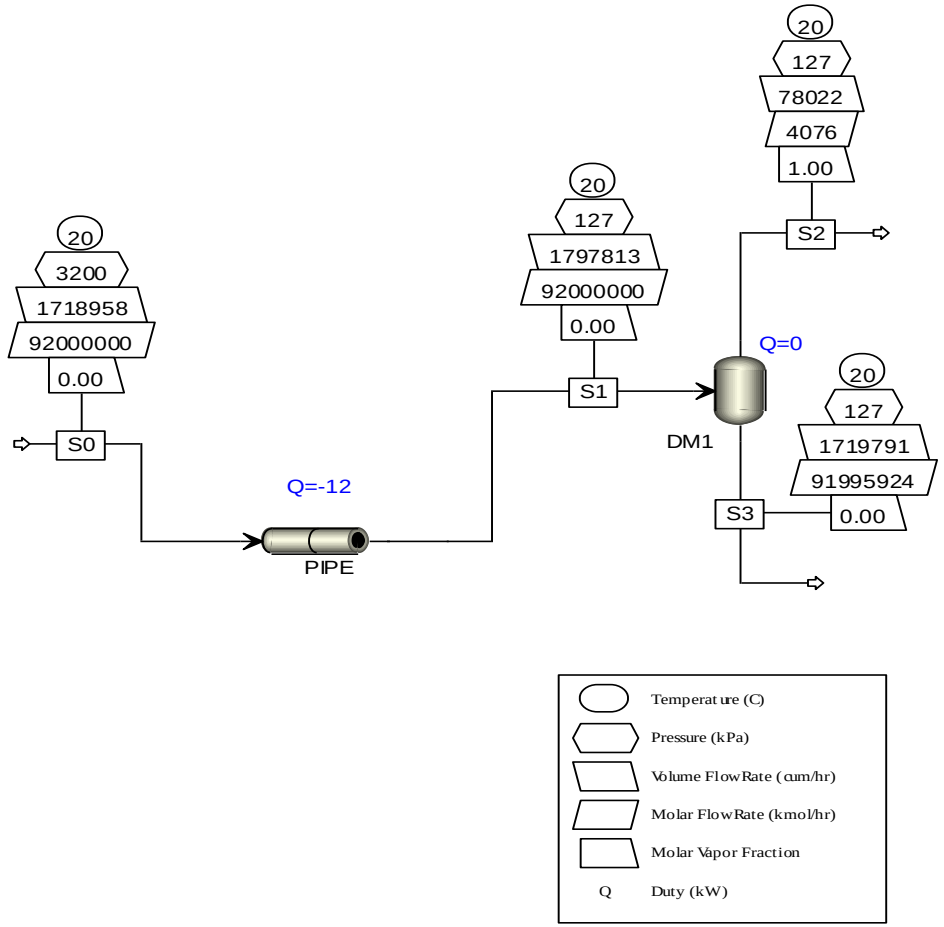

A.2. Absorption

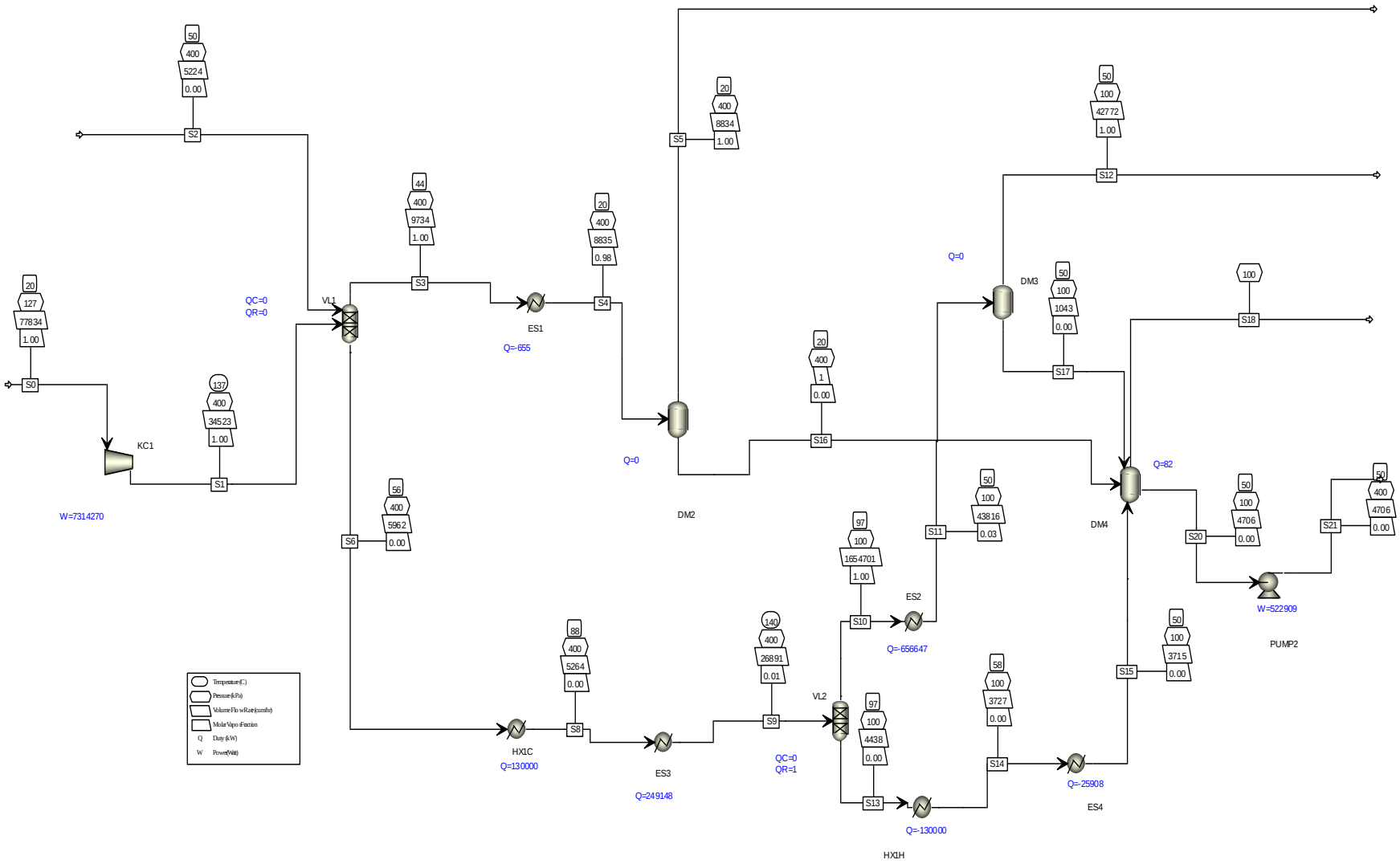

A.2. Adsorption

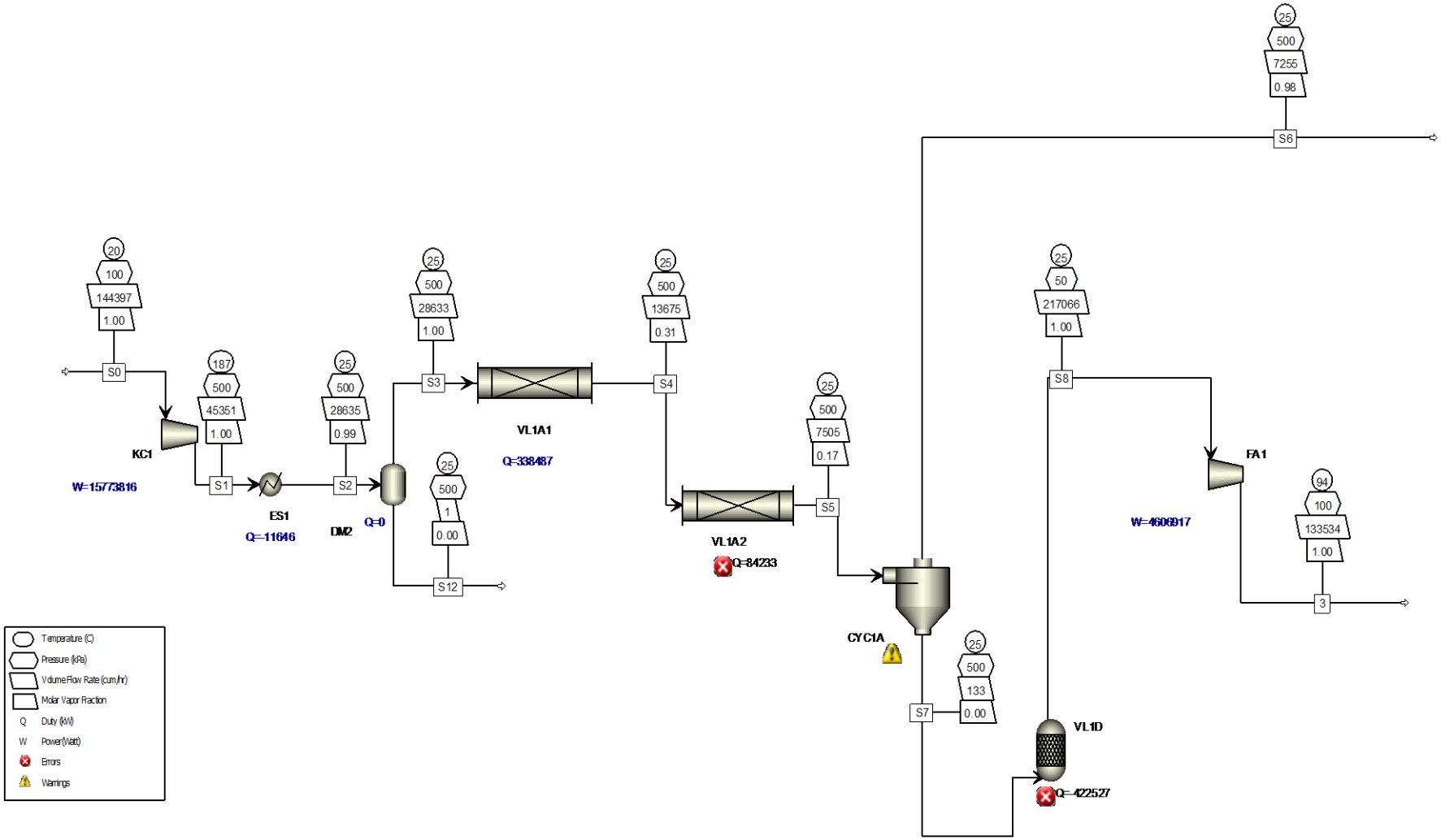

A.3. Cold separation

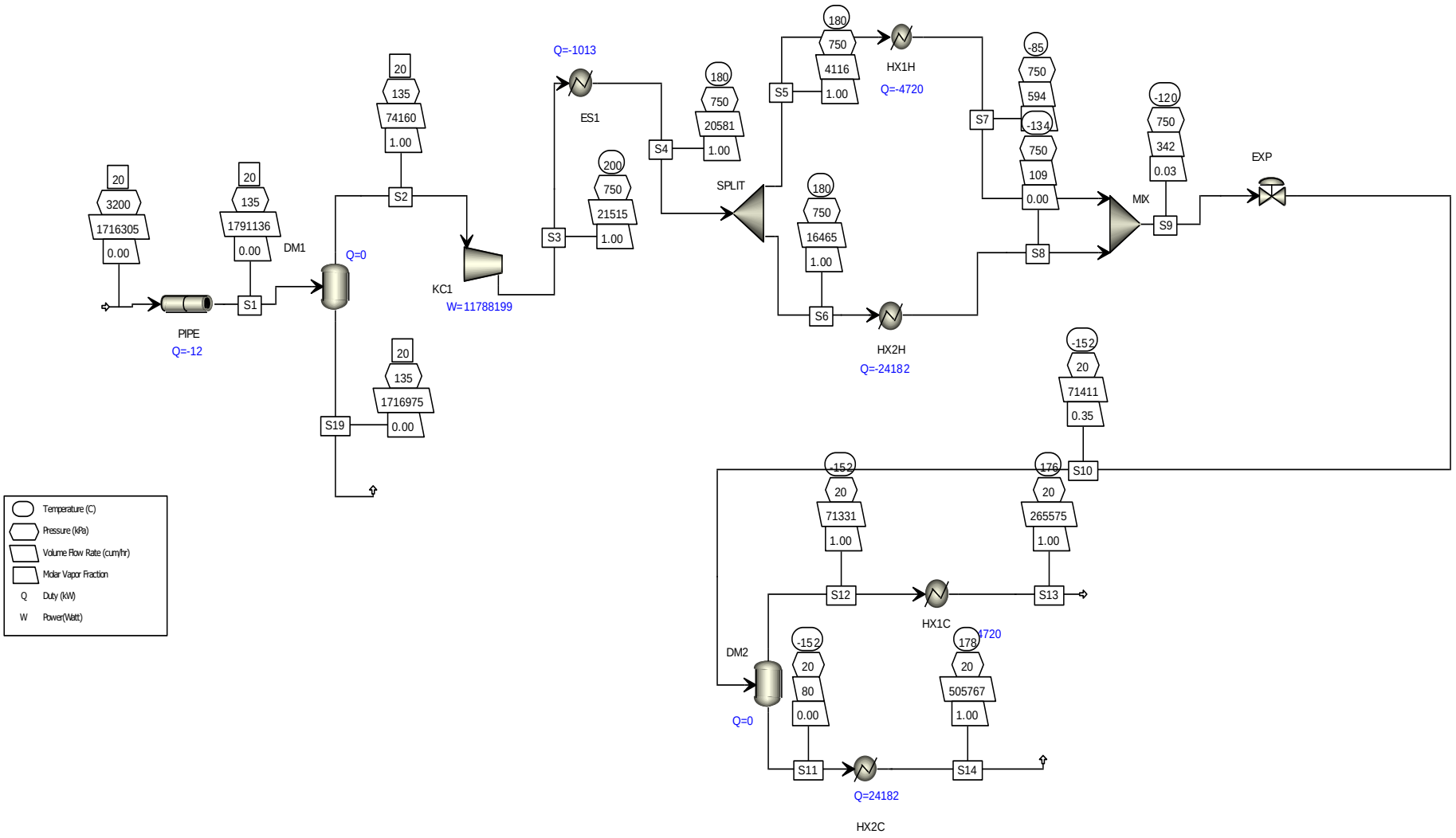

Appendix B –Equipment sizing, estimation of capital costs and operating costs

B.1. Equipment sizing

a. Piping for gas extraction (degassing section)

Results of simulation in Aspen Plus V12 for the degassing section are presented in Appendix A1, the calculated flow rate from the bottom of the Lake is 92 000 000 kmol/hr. This is the molar flow rate required to produce 250 million Nm^3 per year of methane, which is necessary to keep the concentration levels of dissolved gases below the safe level of 16 mmol/l of methane and 80 mmol/l of carbon dioxide. The vertical length of the submerged pipe from the bottom of the Lake to the surface is equal to 320 m, which is the average depth at which dissolved gases are present in water at the bottom of the Lake. A standard diameter for carbon steel piping available is 0.508 m[15]. For a single pipe with a diameter of 0.508 m and a vertical length of 320 m, the calculated flow rate to achieve process conditions in Appendix A1 was found to be 100 000 kmol/hr. This flow rate ensures that the flow regime in the pipe remains in a stable form where the emerging gas is dispersed as fine bubbles in the liquid. To achieve the total flow rate of 92 000 000 kmol/hr, the number of single pipes with diameter of 0.508 m is 920.

b. Gas-liquid separators or flash drums

Horizontal gas-liquid separators are sized by the Souders-Brown method[24]. Values for recommended length to diameter ratios and available diameters are from the online cost estimator for horizontal tanks[15],[24]. Given densities of the liquid and gas streams after separation obtained in Aspen Plus V12, an initial diameter and length of the horizontal drum or tank are selected. The method is then used to calculate the gas velocity required to achieve separation for the case of gas and liquid densities in the flowsheet. A minimum diameter is then calculated based on this gas velocity. If the diameter initially selected is larger than the calculated minimum diameter, the diameter and length initially are retained as suitable to achieve separation. The Souders-Brown procedure is explained in section 5.2.2, paragraph b (Methodology)

Flowsheet	Degassing	Absorption			Adsorption	Cold separation	
Equipment number	DM1	DM2	DM3	DM4	DM2	DM1	DM2
L/D	4	4	4	4	4	4	4
Available diameter	4	4	4	8	4	4	4
Length	16	16	16	16	16	16	16
Ks	0.384541192	0.384541192	0.384541192	0.384541192	0.384541192	0.384541192	0.384541

Gas density	1.759725584	2.699956127	1.523455679	0	6.962359852	1.878089114	0.323952
Liquid density	963.7550097	756.0782545	936.2181208	897.3229811	848.7201392	965.3343237	1450.875
Vg (max)	8.990976566	14.15563467	9.516657843	28.02084757	4.228226117	8.709651266	25.73172
qa (m3/s)	21.67284691	2.454002261	11.48933815	0	7.953611111	20.60027778	19.81417
D (min)	3.082865347	0.955384737	1.239824852	7.528201869	1.547597906	1.73536652	0.990167
D>Dmin check	ok	ok	ok	Ok	ok	ok	ok

c. Compressors

The duty of compressors and fans is reported in the flowsheets of appendix A for each technique of separation. These are results from simulations conducted in Aspen Plus V12 by specifying the required discharge pressure. Referring to Smith et al12, it is assumed that isentropic compression takes place with both an isentropic and mechanical efficiency set at 70%.

Flowsheet	**Absorption**	**Adsorption**		**Cold separation**
Equipment number	**KC1**	**FA1**	**KC1**	**KC1**
Property method	**ENRTL-SR**	**PR-BM**	**ENRTL-RK**	**SRK**
Use true species approach for electrolytes	**YES**	**YES**	**YES**	**YES**
Free-water phase properties method	**STEAM-TA**	**STEAMNBS**	**STEAMNBS**	**STEAM-TA**
Water solubility method	**3**	**3**	**3**	**3**
Model Type	**ISENTROPIC**	**ISENTROPIC**	**ASME-ISENTROP**	**ASME-ISENTROP**
Specified discharge pressure [kPa]	**400**	**100**	**500**	**750**
Isentropic efficiency	**0.7**	**0.7**	**0.7**	**0.7**
Mechanical efficiency	**0.7**	**0.7**	**0.7**	**0.7**
Indicated horsepower [Watt]	5119988.06	3224842.1	11041671.2	8251758.08
Calculated brake horsepower [Watt]	7314268.66	4606917.2	15773816	11788225.8
Net work required [Watt]	7314268.66	4606917.2	15773816	11788225.8
Power loss [Watt]	2194280.6	1382075.2	4732144.8	3536467.75
Efficiency (polytropic / isentropic) used	0.7	0.7	0.7	0.7
Calculated discharge pressure [kPa]	400	100	500	750
Calculated pressure change [kPa]	273	50	400	615.369191
Calculated pressure ratio	3.1496063	2	5	5.57079025

Outlet temperature [C]	136.561845	93.685538	187.436589	199.854268
Isentropic outlet temperature [C]	103.638001	73.7787	140.848356	150.352947
Vapor fraction	1	1	1	1
Head developed [kJ/kg]	93.973646	46.41454	138.885413	149.299156
Isentropic power requirement [Watt]	3583991.64	2257389.5	7729169.84	5776230.66
Inlet heat capacity ratio	1.30186836	1.2928453	1.30068919	1.30323704
Inlet volumetric flow rate [cum/hr]	77834.1998	217066.17	144397.05	74160.6414
Outlet volumetric flow rate [cum/hr]	34523.4629	133533.8	45351.4464	21514.681
Inlet compressibility factor	0.994956235	0.9975999	0.996030695	0.994652947
Outlet compressibility factor	0.994524562	0.9975827	0.995529546	0.996348143
Total feed stream CO2e flow [kg/hr]	694071.241	423747.47	1012790.47	696964.585
Total product stream CO2e flow [kg/hr]	694071.241	423747.47	1012790.47	696964.585
Net stream CO2e production [kg/hr]	0	0	0	0
Utility CO2e production [kg/hr]	0	0	0	0
Total CO2e production [kg/hr]	0	0	0	0

d. Expansion valve

In Aspen Plus V12, the pressure at the outlet of the pressure reduction valve is specified, the simulator then calculates the pressured drop across this valve. A pressure reduction valve was only required for the case of cold separation used as separation technique.

Flowsheet	**Cold separation**
Equipment number	**EXP**
Property method	**SRK**
Use true species approach for electrolytes	**YES**
Free-water phase properties method	**STEAM-TA**
Water solubility method	**3**
Specified outlet pressure [kPa]	**20**
Calculation type	**ADIAB-FLASH**
Valve pressure specification (design mode)	**P-OUT**
EO Model components	

Valve pressure specification (rating mode)	VAL-POSN
Calculated outlet pressure [kPa]	20
Calculated pressure drop [kPa]	730
Piping geometry factor	1
Total feed stream CO2e flow [kg/hr]	696964.585
Total product stream CO2e flow [kg/hr]	696964.585
Net stream CO2e production [kg/hr]	0

e. Separation columns

Separation columns were only necessary for the absorption and adsorption flowsheets.

For the absorption technique, the RADFRAC packed absorption model was used in Aspen Plus V12 to estimate the required number of packed beds (number of equilibrium stages) for absorption of carbon dioxide into the alkaline solution in the first column and the stripping of the carbon dioxide from the alkaline solution in the second column. The cost of the columns in the absorption sheet is then calculated based on this number of packed beds obtained in flowsheets of Appendix A.

Flowsheet	**Absorption**	
Equipment number	**VL1**	**VL2**
Property method	SRK	SRK
Use true species approach for electrolytes	YES	YES
Free-water phase properties method	STEAM-TA	STEAM-TA
Water solubility method	3	3
Number of stages	5	2
Condenser	NONE	NONE
Reboiler	NONE	KETTLE
Number of phases	2	2
Free-water	NO	NO
Top stage pressure [kPa]	400	100
Calculated molar reflux ratio	137.470004	2.87932945
Calculated bottom rate [kmol/hr]	204815.963	152821.744
Calculated boilup rate [kmol/hr]	4200.42652	3422.38838

Calculated distillate rate [kmol/hr]	1487.61048	54194.5967
Condenser / top stage temperature [C]	43.5767118	97.0898537
Condenser / top stage pressure [kPa]	400	100
Condenser / top stage heat duty [kW]	0	0
Condenser / top stage subcooled duty		
Condenser / top stage reflux rate [kmol/hr]	204501.819	156044.098
Condenser / top stage free water reflux ratio		
Reboiler pressure [kPa]	400	100
Reboiler temperature [C]	55.6356707	96.8633713
Reboiler heat duty [kW]	0	1
Total feed stream CO2e flow [kg/hr]	694071.241	17658.2887
Total product stream CO2e flow [kg/hr]	596254.89	114496.468
Net stream CO2e production [kg/hr]	-97816.3514	96838.1798
Utility CO2e production [kg/hr]	0	0
Total CO2e production [kg/hr]	-97816.3514	96838.1798
Basis for specified distillate to feed ratio	**MOLE**	**MOLE**
Basis for specified bottoms to feed ratio	**MOLE**	**MOLE**
Basis for specified boilup ratio	**MOLE**	**MOLE**
Calculated molar boilup ratio		0.022394643
Calculated mass boilup ratio	0.03254676	0.020592575

For the adsorption technique, reactors models were used in Aspen Plus V12 to simulate the adsorption of CO2 in beds of activated carbon, as primary adsorbate, and the desorption of CO2 during regeneration of the activated carbon. Properties of beds of activated carbon have been sourced and derived from results obtained from the various sources (Hauchhum and Mahanta, 2014; Heuchel et al, 1999; Singh and Kumar, 2015). The simulation has produced the length of the packed bed of activated carbon reactor required to achieve adsorption of CO_2 so that the desired flow rate and purity of CH_4 is achieved at the outlet of the packed bed. This length is then used to estimate the mass and the cost of the adsorption bed.

Flowsheet	Adsorption	
Equipment number	VL1A1	VL1A2
Process stream property method	**PR-BM**	**PR-BM**

Process stream use true species approach for electrolytes	**YES**	**YES**
Process stream free-water phase properties method	**STEAMNBS**	**STEAMNBS**
Process stream water solubility method	**3**	**3**
Thermal fluid property method	**PR-BM**	**PR-BM**
Thermal fluid use true species approach for electrolytes	**YES**	**YES**
Thermal fluid free-water phase properties method	**STEAMNBS**	**STEAMNBS**
Thermal fluid water solubility method	**3**	**3**
Reactor dimensions length [meter]	**0.225**	**0.225**
Reactor dimensions diameter [meter]	**3**	**3**
Pressure at reactor inlet: process stream [kPa]	**0**	**0**
Heat duty [kW]	338486.555	84232.8324
Minimum reactor temperature [C]	25.0000001	25.0000001
Maximum reactor temperature [C]	25.0000001	25.0000001
Residence time [sec]	0.159575296	0.656821994
Total feed stream CO2e flow [kg/hr]	1012790.34	876486.439
Total product stream CO2e flow [kg/hr]	876486.439	589042.865
Net stream CO2e production [kg/hr]	-136303.899	-287443.574

f. Pumps

The power requirement for centrifugal pumps was calculated in Aspen Plus V12 and reported in the flowsheets of appendix A. The overall efficiency of centrifugal pump is assumed as 75% (Smith, Van Ness and Abbott)[12]. A pump is only required in the case of absorption used as a technique of separation.

Flowsheet	**Absorption**
Equipment number	**PUMP2**
Property method	**ENRTL-SR**
Use true species approach for electrolytes	**YES**
Free-water phase properties method	**STEAM-TA**
Water solubility method	**3**
Specified discharge pressure [kPa]	**400**
Pump efficiencies	**0.75**
Fluid power [Watt]	392181.97
Calculated brake power [Watt]	522909.293
Electricity [Watt]	522909.293
Volumetric flow rate [cum/hr]	4706.18364
Calculated discharge pressure [kPa]	400
Calculated pressure change [kPa]	300
NPSH available [kJ/kg]	0.071137293
Head developed [kJ/kg]	0.33432778
Pump efficiency used	0.75
Net work required [Watt]	522909.293
Total feed stream CO2e flow [kg/hr]	51455.0848
Total product stream CO2e flow [kg/hr]	51455.0848
Net stream CO2e production [kg/hr]	0
Utility CO2e production [kg/hr]	0
Total CO2e production [kg/hr]	0

g. Heat exchangers

The duty of the heat transfer for every heat exchanger is obtained in the flowsheet models developed in Aspen. The log-mean temperature difference is then calculated for the counter-current flow arrangement. Given the typical ranges for values of the overall heat transfer coefficient reported by Sinnott[11] (Coulson and Richardson, volume 6), the area required for heat transfer is then calculated, results for the three techniques are listed below.

Flowsheet	**Absorption**							
Equipment number	**ES1**	**ES2**	**ES3**	**ES4**	**HX1C**	**HX1H**	**Steam reboiler of VL2**	**Steam heater of DM4**
Property method	**ENRTL-SR**	**ENRTL-SR**	**ENRTL-SR**	**ENRTL-SR**	**ENRTL-SR**	**ENRTL-SR**	**ENRTL-SR**	**ENRTL-SR**
Use true species approach for electrolytes	**YES**	**YES**	**YES**	**YES**	**YES**	**YES**	Refer to results of VL2	Refer to results of DM4
Free-water phase properties method	**STEAM-TA**	**STEAM-TA**	**STEAM-TA**	**STEAM-TA**	**STEAM-TA**	**STEAM-TA**		
Water solubility method	**3**	**3**	**3**	**3**	**3**	**3**		
Specified pressure [kPa]	**0**	**0**	**0**	**0**	**0**	**0**		
Specified temperature [C]	**20**	**50**	**140**	**50**	**140**	**70**		
Specified heat duty [kW]			**1200000**	**0**	**130000**	**-130000**		
Calculated pressure [kPa]	400	100	400	100	400	100		
Calculated temperature [C]	20	50	140	50	88.1650654	58.0236669		
Calculated vapor fraction	0.982483175	0.029508209	0.012517694	0	0	0		
Calculated heat duty [kW]	-655.312861	-656647.402	249147.629	-25908.3062	130000	-130000	1	82
Temperature change [C]							Refer to results of VL2	Refer to results of DM4
Net duty [kW]	-655.312861	-656647.402	249147.629	-25908.3062	0	0		
First liquid / total liquid	1	1	1	1	1	1		

Total feed stream CO2e flow [kg/hr]	578596.601	114304.613	17658.2887	191.855248	17658.2887	191.855248		
Total product stream CO2e flow [kg/hr]	578596.601	114304.613	17658.2887	191.855248	17658.2887	191.855248		
Net stream CO2e production [kg/hr]	0	0	0	0	0	0		
Utility CO2e production [kg/hr]	0	0	0	0	0	0		
Total CO2e production [kg/hr]	0	0	0	0	0	0		
Hot stream inlet temp [C]	44	97	150	58	97	refer to HX1C column	150	150
Cold stream outlet temp [C]	19	19	140	19	88		97	50
Hot stream outlet temp [C]	20	50	150	50	58		150	150
Cold stream inlet temp [C]	19	19	88	19	56		97	50
Flow arrangement	counter-current	counter-current	counter-current	counter-current	counter-current		counter-current	counter-current
DT1 (Hot in - Cold out)	25	78	10	39	9		53	100
DT2 (Hot out - Cold in)	1	31	62	31	2		53	100
Log mean temp difference [C]	7.456019215	50.93627251	28.50018918	34.84708464	4.654015821		53	100
Overall heat transfer coefficient [kW/m2/C]	0.3	1	1	0.8	0.8		1.5	1
Area (m2)	292.9681564	12891.54594	8741.977058	929.3460366	34916.08243		0.012578616	0.82

Flowsheet	**Adsorption**
Equipment number	**ES1**
Property method	**PR-BM**
Use true species approach for electrolytes	**YES**
Free-water phase properties method	**STEAMNBS**

Water solubility method	**3**
Specified pressure [kPa]	**0**
Specified temperature [C]	**25**
Specified heat duty [kW]	**-1000**
Calculated pressure [kPa]	500
Calculated temperature [C]	25
Calculated vapor fraction	0.99077099
Calculated heat duty [kW]	-11646.3395
Temperature change [C]	**-20**
Net duty [kW]	-11646.3395
First liquid / total liquid	1
Total feed stream CO2e flow [kg/hr]	1012790.47
Total product stream CO2e flow [kg/hr]	1012790.47
Net stream CO2e production [kg/hr]	0
Utility CO2e production [kg/hr]	0
Total CO2e production [kg/hr]	0
Hot stream inlet temp [C]	187
Cold stream outlet temp [C]	19
Hot stream outlet temp [C]	25
Cold stream inlet temp [C]	19
Flow arrangement	counter-current
DT1 (Hot in - Cold out)	168
DT2 (Hot out - Cold in)	6
Log mean temp difference [C]	48.61646382
Overall heat transfer coefficient [kW/m2/C]	0.3
Area (m2)	798.5182101

Flowsheet	**Cold separation**				
Equipment number	ES1	HX1C	HX1H	HX2C	HX2H
Property method	**SRK**	**SRK**	**SRK**	**SRK**	**SRK**
Use true species approach for electrolytes	**YES**	**YES**	**YES**	**YES**	**YES**
Free-water phase properties method	**STEAM-TA**	**STEAM-TA**	**STEAM-TA**	**STEAM-TA**	**STEAM-TA**

Water solubility method	**3**	**3**	**3**	**3**	**3**
Specified pressure [kPa]	**0**	**0**	**0**	**0**	**0**
Specified temperature [C]	**0**	**-120**	**-120**	**-45**	**-119**
Specified heat duty [kW]	**-1000**	**4720**	**-4700**	**24182**	**-24200**
Calculated pressure [kPa]	750	20	750	20	750
Calculated temperature [C]	179.854268	176.205292	-85.1457324	178.147429	-134.145732
Calculated vapor fraction	1	1	0.362427642	1	0
Calculated heat duty [kW]	-1012.86828	4720	-4720.33005	24182	-24181.5949
Temperature change [C]	**-20**		**-265**		**-314**
Net duty [kW]	-1012.86828	0	-4720.33005	0	-24181.5949
First liquid / total liquid			1		1
Total feed stream CO2e flow [kg/hr]	696964.585	566374.143	139392.917	130590.442	557571.668
Total product stream CO2e flow [kg/hr]	696964.585	566374.143	139392.917	130590.442	557571.668
Net stream CO2e production [kg/hr]	0	0	0	0	0
Utility CO2e production [kg/hr]	0	0	0	0	0
Total CO2e production [kg/hr]	0	0	0	0	0
Hot stream inlet temp [C]	200	Refer to HX1H column	180	Refer to HX2C column	180
Cold stream outlet temp [C]	19		176		178
Hot stream outlet temp [C]	180		-85		-34
Cold stream inlet temp [C]	19		-152		-134
Flow arrangement	counter-current		counter-current		counter-current
DT1 (Hot in - Cold out)	181		4		2
DT2 (Hot out - Cold in)	161		67		100
Log mean temp difference [C]	170.8048901		22.35312196		25.05097743
Overall heat transfer coefficient [kW/m2/C]	1		0.01		0.01
Area (m2)	1.052980789		380.9120379		535.4910099

B.2. Estimation of equipment purchase costs

Equipment purchase costs

The purchase cost of process equipment is estimated using the technique as recommended as described by Sinnott[11]; and Peters and Timmerhaus[14], [15]. An equation is given for each type of equipment for a selected range of size or capacity. These are the equations used to estimate the purchased cost of each piece of equipment with the year 2002 as basis of reference for cost inflation. The chemical plant cost index (CEPCI) published by the Chemical Engineering journal was used as the index for cost inflation over time in this research[15].

a. Degassing section

Degassing section	Size (S)	Unit	Quantity (n)	Equation	a	b	Equipment cost ($) (2002, CEPCI = 390.4)	Equipment cost ($) (2022, CEPCI = 877.5)
Degassing piping LN1. 0.508 m diameter	320	M	920	a*(n*S)	128.538	n/a	$37,841,440	$85,056,003
Degassing drum, DM1 Diameter: 4 m	16	M	1	(a*S+b)*n	12291	50577	$247,233	$555,704

b. Gas-liquid separators or horizontal stainless steel drums

Equipment	Separation Technique	Size (S)	Unit	Quantity (n)	Equation	a	b	Equipment cost ($) (2002, CEPCI = 390.4)	Equipment cost ($) (2022, CEPCI = 877.5)
Drums DM2	Absorption	16	m	1	(a*S+b)*n	12291	50577	$247,233	$555,704
Drums DM3	Absorption								
Drums DM4	Absorption								
Drums DM2	Adsorption								
Drums DM1	Cold separation								
Drums DM2	Cold separation								

c. Compressors

Equipment	Separation Technique	Size (S)	Unit	Quantity (n)	Equation	a	b	Equipment cost ($) (2002, CEPCI = 390.4)	Equipment cost ($) (2022, CEPCI = 877.5)
Compressors,KC1	Absorption	6000	kW	2	a*n*(+)	2193.2	0.947671945	$16,099,184	$36,186,050
Compressors,KC1	Adsorption	6000		3		2193.2	0.94983738	$24,148,776	$54,279,075
Compressors,KC1	Cold separation	6000		2		2193.2	0.947671945	$16,099,184	$36,186,050

d. Expansion valve

Equipment	Separation Technique	Size (S)	Unit	Quantity (n)	Equation	a	b	c	Equipment cost ($) (2002, CEPCI = 390.4)	Equipment cost ($) (2022, CEPCI = 877.5)
Expansion valve, EXP	Cold separation	0.305	m	1	[a*(S^2)+b*S+c]*n	139255	8071.3	1018.9	$16,435	$36,941

e. Blowers

Equipment	Separation Technique	Size (S)	Unit	Quantity (n)	Equation	a	b	Equipment cost ($) (2002, CEPCI = 390.4)	Equipment cost ($) (2022, CEPCI = 877.5)
Blowers, FA1	Adsorption	4.72	m3/s	13	a*(S^b)*n	45868	0.616000846	$1,550,965	$3,486,096

f. Separation columns

Equipment	Separation Technique	Size (S)	Unit	Quantity (n)	Equation	a	b	c	Equipment cost ($) (2002, CEPCI = 390.4)	Equipment cost ($) (2022, CEPCI = 877.5)
Absorption columns, VL1	Absorption	6	m	1	(a*S+b)*n	18291	86158	n/a	$195,904	$440,332
Ceramic packing in VL1	Absorption	6	m	1	(a*S+b)*n	5474	3454	n/a	$36,298	$81,587
Stripping columns, VL2	Absorption	6	m	1	(a*S+b)*n	18291	86158	n/a	$195,904	$440,332
Ceramic packing in VL2	Absorption	6	m	1	(a*S+b)*n	5474	3454	n/a	$36,298	$81,587
Adsorption columns, VLA1	Adsorption	0.225	m	10	(a*S+b)*n	71317	-31.625	n/a	$160,147	$359,962
Adsorption columns, VLA2	Adsorption	0.225	m	10	(a*S+b)*n	71317	-31.625	n/a	$160,147	$359,962
Activated carbon in VLA1 & VLA2	Adsorption	5.6	ton	1	a*S*n	3000	n/a	n/a	$16,800	$37,761

g. Pumps

Equipment	Separation Technique	Size (S)	Unit	Quantity (n)	Equation	a	b	Equipment cost ($) (2002, CEPCI = 390.4)	Equipment cost ($) (2022, CEPCI = 877.5)
Pumps PC1	Absorption	174	kW	3	a*exp(b*S)*n	8870.3	0.012417708	$230,904	$519,002

h. Heat exchangers

Equipment	Separation Technique	Size (S)	Unit	Quantity (n)	Equation	a	b	c	Equipment cost ($) (2002, CEPCI = 390.4)	Equipment cost ($) (2022, CEPCI = 877.5)
Heat exchangers, rich solvents-lean solvent, HX1	Absorption	1000	m2	35	[a*(S^2)+b*S+c]*n	-0.0485	234.41	15220	$7,039,550	$15,822,759
Absorption columns overhead gas condensers, ES1	Absorption	293	m2	1	[a*(S^2)+b*S+c]*n	-0.03998	234.41	15220	$80,470	$180,872
Stripping columns overhead gas condensers, ES2	Absorption	1000	m2	13	[a*(S^2)+b*S+c]*n	-0.0485	234.41	15220	$2,614,690	$5,877,025
Stripping columns feed heaters, ES3	Absorption	1000	m2	9	[a*(S^2)+b*S+c]*n	-0.0485	234.41	15220	$1,810,170	$4,068,709
Lean solvent from stripping	Absorption	929	m2	1	[a*(S^2)+b*S+c]*n	-0.05299	234.41	15220	$187,254	$420,890

columns coolers, ES4										
Stripping columns reboilers, ES5	Absorption	9.3	m2	1	[a*(S^2)+b*S+c]*n	-0.05299	234.41	9802.57014	$11,978	$26,923
Mixing tank heaters, ES6	Absorption	9.3	m2	1	[a*(S^2)+b*S+c]*n	-0.05299	234.41	9802.57014	$11,978	$26,923
Feed coolers, ES1	Adsorption	799	m2	1	[a*(S^2)+b*S+c]*n	-0.05962	234.41	15220	$164,452	$369,638
Heat exchanger, HX1	Cold separation	1000	m2	22	[a*(S^2)+b*S+c]*n	-0.0485	234.41	15220	$4,424,860	$9,945,734
Heat exchanger, HX2	Cold separation	1000	m2	97	[a*(S^2)+b*S+c]*n	-0.0485	234.41	15220	$19,509,610	$43,851,646
Cooler, ES1	Cold separation	9.3	m2	1	[a*(S^2)+b*S+c]*n	-0.05299	234.41	9802.57014	$11,978	$26,923

B.3. Estimation of annual operating costs

Year	Total capital investment	Net cash flow	Discounted net cash flow
0	$824,574,529	$0	$0
1		$304,281,531	$223,040,061
2		$304,281,531	$163,489,611
3		$304,281,531	$119,838,798
4		$304,281,531	$87,842,508
5		$304,281,531	$64,389,049
6		$304,281,531	$47,197,532
7		$304,281,531	$34,596,055
8		$304,281,531	$25,359,101
9		$304,281,531	$18,588,363

10		$304,281,531	$13,625,374
11		$304,281,531	$9,987,475
12		$304,281,531	$7,320,875
13		$304,281,531	$5,366,242
14		$304,281,531	$3,933,486
IR	**Check**		
36%	0.000103116		

B.4. Estimation of Capital and Operating costs for Cold Separation flowsheet

Year	Total capital investment	Net cash flow	Discounted net cash flow
0	$1,005,218,826	$0	$0
1		$316,123,084	$241,854,511
2		$316,123,084	$185,034,271
3		$316,123,084	$141,563,129
4		$316,123,084	$108,304,907
5		$316,123,084	$82,860,226
6		$316,123,084	$63,393,408
7		$316,123,084	$48,500,038
8		$316,123,084	$37,105,651
9		$316,123,084	$28,388,212
10		$316,123,084	$21,718,810
11		$316,123,084	$16,616,288
12		$316,123,084	$12,712,530
13		$316,123,084	$9,725,904
14		$316,123,084	$7,440,942
IR	Check		
31%	5.60284E-06		

Appendix C – Calculations of internal rate of return

C.1. Interpolation of Chemical Plant Cost Index for year 2022

Year	CE plant cost index
2008	575.4
2009	521.9
2010	550.8
2011	585.7
2012	584.6
2013	567.3
2014	579.8
2015	556.8
2020	594.1
2021	735.8
2022	877.5

C.2. Calculations of internal rate of return for Absorption flowsheet

Year	Total capital investment	Net cash flow	Discounted net cash flow
0	$860,625,945	$0	$0
1		$264,210,283	$203,375,232
2		$264,210,283	$156,547,598
3		$264,210,283	$120,502,138
4		$264,210,283	$92,756,232
5		$264,210,283	$71,398,888
6		$264,210,283	$54,959,123
7		$264,210,283	$42,304,653
8		$264,210,283	$32,563,905
9		$264,210,283	$25,065,988
10		$264,210,283	$19,294,484
11		$264,210,283	$14,851,883
12		$264,210,283	$11,432,201
13		$264,210,283	$8,799,910
14		$264,210,283	$6,773,709
IR	Check		
30%	3.93391E-06		

C.3. Calculations of internal rate of return for Adsorption flowsheet

Year	Total capital investment	Net cash flow	Discounted net cash flow
0	$824,574,529	$0	$0
1		$304,281,531	$223,040,061
2		$304,281,531	$163,489,611
3		$304,281,531	$119,838,798
4		$304,281,531	$87,842,508
5		$304,281,531	$64,389,049
6		$304,281,531	$47,197,532
7		$304,281,531	$34,596,055
8		$304,281,531	$25,359,101
9		$304,281,531	$18,588,363
10		$304,281,531	$13,625,374
11		$304,281,531	$9,987,475
12		$304,281,531	$7,320,875
13		$304,281,531	$5,366,242
14		$304,281,531	$3,933,486
IR	Check		
36%	0.000103116		

C.4. Calculations of internal rate of return for Cold Separation flowsheet

Year	Total capital investment	Net cash flow	Discounted net cash flow
0	$1,005,218,826	$0	$0
1		$316,123,084	$241,854,511
2		$316,123,084	$185,034,271
3		$316,123,084	$141,563,129
4		$316,123,084	$108,304,907
5		$316,123,084	$82,860,226
6		$316,123,084	$63,393,408
7		$316,123,084	$48,500,038
8		$316,123,084	$37,105,651
9		$316,123,084	$28,388,212
10		$316,123,084	$21,718,810
11		$316,123,084	$16,616,288
12		$316,123,084	$12,712,530
13		$316,123,084	$9,725,904
14		$316,123,084	$7,440,942
IR	Check		
31%	5.60284E-06		